

A Design of Low-Projection SCMA Codebooks for Downlink Satellite Internet of Things

Qu Luo, Zilong Liu, *Senior Member, IEEE*, Gaojie Chen, *Senior Member, IEEE*, Pei Xiao, *Senior Member, IEEE*, Yi Ma, *Senior Member, IEEE* and Amine Maaref, *Senior Member, IEEE*.

Abstract—This paper presents a systematic investigation on codebook design of sparse code multiple access (SCMA) communication in downlink satellite Internet-of-Things (S-IoT) systems that are generally characterized by Rician fading channels. To serve a huge number of low-end IoT sensors, we aim to develop enhanced SCMA codebooks which enable ultra-low decoding complexity, while achieving good error performance. By analysing the pair-wise probability in Rician fading channels, we deduce the design metrics for multi-dimensional constellation construction and sparse codebook optimization. To reduce the decoding complexity, we advocate the key idea of projecting the multi-dimensional constellation elements to a few overlapped complex numbers in each dimension, called low projection (LP). We consider golden angle modulation (GAM), thus the resultant multi-dimensional constellation is called LPGAM. With the proposed design metrics and based on LPGAM, we propose an efficient approach of multi-stage optimization of sparse codebooks. Numerical and simulation results show the superiority of the proposed LP codebooks (LPCBs) in terms of decoding complexity and error rate performance. In particular, some of the proposed LPCBs can reduce the decoding complexity by 97% compared to the conventional codebooks, and own the largest minimum Euclidean distance among existing codebooks. The proposed LPCBs are available at <https://github.com/ethanlq/SCMA-codebook>.

Index Terms—Sparse code multiple access (SCMA), codebook design, satellite Internet of Things (S-IoT), low complexity detection.

I. INTRODUCTION

IN recent years, satellite Internet of Thing (S-IoT) has attracted tremendous research attention targeting for providing ubiquitous coverage for massive machine-type communication (mMTC) devices even in remote areas lacking of terrestrial network infrastructure [1]–[3]. With the increasingly scarce and congested spectrum, it is challenging to support the concurrent communications of these MTC devices (which are often low-end S-IoT sensors) with stringent constraints in terms of battery life and computation/storage capabilities [4], [5]. Due the limited time-frequency resources, legacy orthogonal multiple access (OMA) may no longer applicable. A disruptive technique for addressing such a challenge is called non-orthogonal multiple access (NOMA) which permits several times of MTC devices larger than that in OMA systems communicating simultaneously.

Qu Luo, Gaojie Chen, Pei Xiao and Yi Ma are with 5G & 6G Innovation Centre, University of Surrey, UK, email:{q.u.luo, gaojie.chen, p.xiao, m.yi}@surrey.ac.uk.

Zilong Liu is with the School of Computer Science and Electronics Engineering, University of Essex, UK, email: zilong.liu@essex.ac.uk.

Amine Maaref is with the Canada Research Center, Huawei Technologies Company Ltd., Ottawa, Canada, email: amine.maaref@huawei.com.

Existing NOMA techniques can be mainly categorized into two classes: power-domain NOMA [6] and code-domain NOMA (CD-NOMA) [7]. The former advocates the superposition of multiple users with distinctive power levels over the identical time-frequency resources, whereas the latter carries out multiplexing by employing carefully designed codebooks/sequences. This paper focuses on the sparse code multiple access (SCMA) [8], [9], which is a representative CD-NOMA scheme with sparse codebooks. In SCMA, every user’s instantaneous input message bits are directly mapped to a multi-dimensional sparse codeword drawn from a pre-designed codebook [10]. SCMA is attractive as judiciously designed codebooks lead to constellation shaping gain, whilst their sparsity can be leveraged to enable near-optimum low-complexity message passing (MPA) decoding [9].

Many studies have been carried out to reap the benefits of SCMA in supporting massive connectivity. The random access (RA) of SCMA for IoT networks has been studied in [11], [12], which shows the feasibility of the SCMA-based RA procedure in supporting massive connectivity. To reduce the signaling overhead and access delay in the RA process, grant-free SCMA has been further investigated. Specifically, [13] introduced a novel uplink grant-free asynchronous flipped SCMA scheme for future S-IoT communication networks. The error performance of grant-free SCMA under codebook collision was analyzed in [14]. Moreover, [15] proposed an SCMA based secure communication scheme for satellite communication from codebook design point of view.

To deploy SCMA in S-IoT networks, it is pivotal to design good sparse codebooks to permit excellent decoding error performance [16] and ultra-low decoding complexity [17]. A comprehensive survey on various multidimensional constellations for uplink SCMA codebook design was given in [18]. In downlink SCMA, one may apply certain user-specific operations (e.g., interleaving, permutation, shuffling and phase rotations) to a common multidimensional constellation, called a mother constellation (MC), for multiple sparse codebooks [8], [16]. Following this approach, various types of SCMA codebooks have been developed in [19]–[30]. By looking into the pairwise error probability (PEP) of a single-user error event over different channel conditions, it is desirable to maximize the minimum product distance (MPD) or minimum Euclidean distance (MED) of an MC [19]–[23]. In general, a large MED leads to reliable detection in the Gaussian channel, whereas a large MPD is preferred for robust transmissions in the Rayleigh fading channel [31], [32]. For example, the authors in [20] proposed a simple constellation rotation and interleaving

based codebook design scheme based on an MC with enlarged MED. Golden angle modulation (GAM) constellation was adopted in [21] to construct SCMA codebooks with low peak-to-average power ratio properties.

In [26], Star-QAM based MC has been proposed for downlink SCMA. Genetic algorithm was employed to maximize the MED of the superimposed codewords in [27]. In addition, a uniquely decomposable constellation group based codebook design approach was proposed in [28] by maximizing the MED at each resource node. A novel class of power-imbalanced SCMA codebooks has been developed in [29] by maximizing the MED of the superimposed codewords whilst maintaining a large MPD of the MC. Downlink quaternary sparse codebooks with large MED were obtained in [33] by solving a non-convex optimization problem.

It is worth mentioning that the complexity of MPA decoding can be significantly reduced by designing an MC with low projection (LP) numbers [34], [35], which allows overlapped constellation elements at the same dimension. The rationale is that, due to the multidimensional nature, any two MC vectors with certain overlapping dimension may be well separated in other dimensions. Importantly, constellation overlapping at certain dimension leads to less computations in the message passing based inference. The authors in [34] showed that by properly choosing the MC and the LP number, the MPA receiver can utilise the constellation structure to reduce the number of calculations of belief messages at each iteration. Subsequently, [35] presented an LP codebook design based on the amplitude phase-shift keying constellation in each dimension in bit-interleaved coded modulation (BICM) SCMA systems in uplink Rayleigh fading channels.

A. Motivations and contributions

It is noted that the MTC devices in a downlink S-IoT network are usually low-end wireless sensor devices which have very limited battery life and computation/storage capabilities. Thus, the corresponding MPA decoding should have extremely low complexity and super-rapid convergence rate. This is in sharp contrast to the LP codebook design in [34] and [35] for uplink SCMA channels where the decoding is carried out at an advanced base-station receiver. Furthermore, the codebook design in downlink channels needs to deal with the difficulties for joint optimization of the MC and user-specific codebook operators as well as the prohibitively high computational complexity in calculating the MED of the superimposed codewords.

In spite of numerous SCMA codebook designs for Gaussian channels or Rayleigh fading channels, they may not be optimal for satellite-to-terrestrial channels, each often characterized by a Rician fading channel with a line-of-sight (LOS) propagation component [36]–[38]. These motivate us to design enhanced codebooks that can substantially reduce the decoding complexity, while achieving good error performance for downlink S-IoT networks under Rician fading channels.

The main contributions of this work are summarized as follows:

- We analyze the system performance in downlink S-IoT network, and derive the minimum distance of the

superimposed codewords in the Rician fading channel by analyzing and minimizing the conditional PEP. We show that derived minimum distance also generalize the previous designed metric in the AWGN and Rayleigh fading channels, i.e., the MED and MPD, respectively.

- We propose a novel class of LP codebook (LPCB) to enable low complexity detection. Specifically, an efficient algorithm to construct the one-dimensional basic constellation with proper LP numbers based on golden angle modulation¹ (LPGAM) is first proposed. Based on the proposed LPGAM, a general multi-stage scheme is then developed to construct multiple sparse codebooks by optimizing the MC, constellation operators, and bit labeling.
- We study the SCMA systems with both large codebook size and overloading factor, which are more challenging design cases. Extensive simulations are also conducted to evaluate the proposed codebooks in different S-IoT scenarios. We show that the decoding can be performed in a single shot for some of the proposed LPCBs, and thus the decoding complexity for these LPCBs is dramatically reduced. In addition, to our best knowledge, some of the proposed LPCBs also achieve the largest MED values among all existing codebooks.

B. Organization

The rest of the paper is organized as follows. In Section II, the system model of downlink SCMA along with the multiuser detection technique are presented. Section III analyzes the PEP of SCMA system in Rician fading channels and derive the criteria of codebook design. In Section IV, the proposed codebook design and optimization is elaborated. The numerical results are given in Section V. Finally, conclusions are made in Section VI.

C. Notations

$\mathbb{C}^{k \times n}$ and $\mathbb{B}^{k \times n}$ denote the $(k \times n)$ -dimensional complex and binary matrix spaces, respectively. Z_M stands for the integer set $\{1, 2, \dots, M\}$. $\lfloor \cdot \rfloor$, $|\cdot|$ and $\|\cdot\|$ denote the floor function, absolute value, and the ℓ_2 -norm, respectively. $\mathcal{CN}(0, 1)$ denotes complex Gaussian distribution with zero-mean and unit-variance. $\text{diag}(\cdot)$ denotes the diagonalization of a matrix.

II. SYSTEM MODEL

A. System Model

We consider an SCMA system in a satellite-enabled IoT network, where the satellite serves multiple SCMA user groups², as shown in Fig. 1. Each SCMA user group consists of J IoT users (or devices) occupying K orthogonal resource nodes, and the overloading factor is defined as $\lambda = \frac{J}{K} > 1$. At the

¹Golden angle modulation is an emerging modulation that leads to higher mutual information performance and lower peak-to-average power ratio (PAPR) performance over pulse-amplitude modulation and square quadrature amplitude modulation (QAM) [39]

²These users in the same group generally have similar locations, and the detailed user grouping scheme is beyond the scope of this paper.

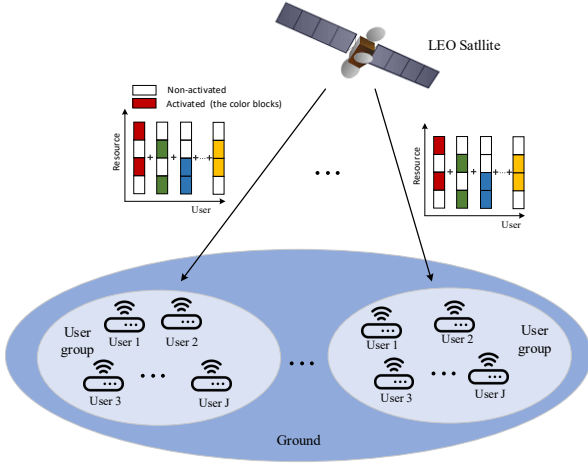


Fig. 1: SCMA system model in an S-IoT network.

satellite side, the SCMA encoder maps $\log_2(M)$ binary bits to a length- K codeword \mathbf{x}_j drawn from pre-defined codebook $\mathcal{X}_j \in \mathbb{C}^{K \times M}$, where M denotes the modulation order. The mapping process is defined as

$$f_j: \mathbb{B}^{\log_2 M \times 1} \rightarrow \mathcal{X}_j \in \mathbb{C}^{K \times M}, \text{ i.e., } \mathbf{x}_j = f_j(\mathbf{b}_j), \quad (1)$$

where $\mathcal{X}_j = \{\mathbf{x}_{j,1}, \mathbf{x}_{j,2}, \dots, \mathbf{x}_{j,M}\}$ is the codebook set for the j th user with cardinality of M and $\mathbf{b}_j = [b_{j,1}, b_{j,2}, \dots, b_{j,\log_2 M}]^T \in \mathbb{B}^{\log_2 M \times 1}$ stands for the j th user's incoming binary message vector. The K -dimensional complex codewords in the SCMA codebook are sparse vectors with N non-zero elements and $N < K$. Let \mathbf{c}_j be a length- N vector drawn from $\mathcal{C}_j \subset \mathbb{C}^{N \times M}$, where \mathcal{C}_j is obtained by removing all the zero elements in \mathcal{X}_j . We further define the mapping from $\mathbb{B}^{\log_2 M}$ to \mathcal{C}_j as [40]

$$g_j: \mathbb{B}^{\log_2 M \times 1} \mapsto \mathcal{C}_j, \text{ i.e., } \mathbf{c}_j = g_j(\mathbf{b}_j). \quad (2)$$

Thus, the SCMA mapping defined in (1) now can be rewritten as

$$f_j \equiv \mathbf{V}_j g_j, \text{ i.e., } \mathbf{x}_j = \mathbf{V}_j g_j(\mathbf{b}_j), \quad (3)$$

where $\mathbf{V}_j \in \mathbb{B}^{K \times N}$ is a mapping matrix that maps the N -dimensional vector to a K -dimensional sparse SCMA codeword³. The sparse structure of the J SCMA codebooks can be represented by an indicator (sparse) matrix $\mathbf{F}_{K \times J} = [\mathbf{f}_1, \dots, \mathbf{f}_J] \subset \mathbb{B}^{K \times J}$ where $\mathbf{f}_j = \text{diag}(\mathbf{V}_j \mathbf{V}_j^T)$. The variable node j is connected to resource node k if and only if $f_{k,j} = 1$. Furthermore, let $\mathcal{I}_r(k) = \{j | f_{k,j} = 1\}$ and $\mathcal{I}_u(j) = \{k | f_{k,j} = 1\}$ are the set of user indices sharing resource node k and the set of resource indices occupied by user j , respectively. In this paper, the following two factor indicator matrices with $\lambda = 150\%$ and $\lambda = 200\%$ are employed:

$$\mathbf{F}_{4 \times 6} = \begin{bmatrix} 0 & 1 & 1 & 0 & 1 & 0 \\ 1 & 0 & 1 & 0 & 0 & 1 \\ 0 & 1 & 0 & 1 & 0 & 1 \\ 1 & 0 & 0 & 1 & 1 & 0 \end{bmatrix}, \quad (4)$$

³For user j , the N non-zero element positions remain unchanged from one codeword to another.

$$\mathbf{F}_{5 \times 10} = \begin{bmatrix} 1 & 1 & 1 & 1 & 0 & 0 & 0 & 0 & 0 & 0 \\ 1 & 0 & 0 & 0 & 1 & 1 & 1 & 0 & 0 & 0 \\ 0 & 1 & 0 & 0 & 1 & 0 & 0 & 1 & 1 & 0 \\ 0 & 0 & 1 & 0 & 0 & 1 & 0 & 1 & 0 & 1 \\ 0 & 0 & 0 & 1 & 0 & 0 & 1 & 0 & 1 & 1 \end{bmatrix}. \quad (5)$$

In the downlink channel, J users' data are first superimposed at the base station and then transmitted over K orthogonal subcarriers. The received signal of user u can be expressed as

$$\mathbf{y}_u = \text{diag}(\mathbf{h}_u) \sum_{j=1}^J \mathbf{x}_j + \mathbf{n}_u, \quad (6)$$

where $\mathbf{h}_u = [h_{u,1}, h_{u,2}, \dots, h_{u,K}]^T \in \mathbb{C}^{K \times 1}$ denotes channel coefficient vector between the satellite and u th IoT user. In general, the satellite-to-terrestrial channels can be modeled as Rician fading channels [36]–[38]. Namely, $h_{u,k} \sim \mathcal{CN}\left(\sqrt{\frac{\kappa}{1+\kappa}}, \sqrt{\frac{1}{1+\kappa}}\right)$ with κ represents the ratio of average power in the LOS path over that in the scattered component. The probability density function of the normalized Rician random variable is given by [41]

$$f_{|h_{u,k}|}(x) = 2x(1+\kappa) \exp(-\kappa - x^2(1+\kappa)) \cdot I_0\left(2x\sqrt{\kappa(1+\kappa)}\right), \quad x \geq 0,$$

where $I_0(\cdot)$ is the first order modified Bessel function of the first kind. For simplicity of analysis, we assume the K subcarriers follow the same Rician distribution of κ . $\mathbf{n}_u = [n_{u,1}, n_{u,2}, \dots, n_{u,K}]^T$ is the complex additive white Gaussian noise vector each element of which has zero mean and variance N_0 , i.e., $n_{u,k} \sim \mathcal{CN}(0, N_0)$. For simplicity, hereafter the subscript u is omitted throughout this paper.

B. SCMA Detection

Similar to many previous works, we assume that the channel state information is perfectly known by receiver. Thanks to the sparsity property of the SCMA codewords, the MPA detector is applied to reduce the decoding complexity. Define $I_{r_k \rightarrow u_j}^{(t)}(\mathbf{x}_j)$ as the belief message associated with codewords \mathbf{x}_j which is transmitted from resource node r_k to variable node u_j at the t th iteration. Similar, denoted by $I_{u_j \rightarrow r_k}^{(t)}(\mathbf{x}_j)$ the belief message from variable node u_j to resource node r_k . The iterative messages exchanged between resource nodes and variable nodes are computed as

$$\begin{aligned} & I_{r_k \rightarrow u_j}^{(t)}(\mathbf{x}_j) \\ &= \sum_{\substack{\mathbf{x}_j = \mathbf{x} \\ i \in \mathcal{I}_r(k) \setminus \{j\} \\ \mathbf{x}_i \in \mathcal{X}_i}} \frac{1}{\pi N_0} \exp\left\{-\frac{|y_k - h_k \sum_{i \in \mathcal{I}_r(k)} x_{k,i}|^2}{N_0}\right\} \\ & \quad \times \prod_{i \in \mathcal{I}_r(k) \setminus \{j\}} I_{u_i \rightarrow r_k}^{(t-1)}(\mathbf{x}_i), \end{aligned} \quad (7)$$

and

$$I_{u_j \rightarrow r_k}^{(t)}(\mathbf{x}_j) = \alpha_j \times \prod_{\ell \in \mathcal{I}_u(j) \setminus \{k\}} I_{r_\ell \rightarrow u_j}^{(t-1)}(\mathbf{x}_j), \quad (8)$$

where α_j is a normalization factor. We assume equal probability for the input message \mathbf{x}_j , i.e.,

$$I_{r_k \rightarrow u_j}^{(0)}(\mathbf{x}_j) = \frac{1}{M}, \forall j = 1, \dots, J, \forall k \in \mathcal{I}_u(j). \quad (9)$$

At each iteration, the main complexity of MPA is dominated by the message updating at the resource node, which can be approximated as $\mathcal{O}(KM^{d_f})$, where d_f is the number of users which collide over a resource node. To reduce the decoding complexity of MPA at each iteration, one possible approach is to reduce the effective M for the codebook, which is the key idea of the proposed LPCBs.

III. PROPOSED DESIGN CRITERIA OF SPARSE CODEBOOK IN DOWNLINK RICIAN CHANNELS

In this section, we first analyze the PEP performance of SCMA in the downlink Rician channel. We show that the PEPs in AWGN and Rayleigh fading channels can be regarded as two special cases of that of Rician fading channels. Then, we present the corresponding design criteria.

A. PEP analysis in downlink Rician fading channels

In downlink SCMA systems, users' data are first superimposed over K orthogonal resources, which constitute superimposed constellation Φ_{MJ} . Let $\mathbf{w} = \sum_{j=1}^J \mathbf{x}_j$ be a superimposed codeword of Φ_{MJ} . Assume the erroneously decoded codeword is $\hat{\mathbf{w}}$ when \mathbf{w} is transmitted, where $\mathbf{w}, \hat{\mathbf{w}} \in \Phi_{MJ}$, and $\mathbf{w} \neq \hat{\mathbf{w}}$. Furthermore, Let us define the element-wise distance $\tau_{\mathbf{w} \rightarrow \hat{\mathbf{w}}}(k) = \left| \sum_{j \in \mathcal{I}_r(k)} (x_{j,k} - \hat{x}_{j,k}) \right|^2$ and Euclidean distance $\delta_{\mathbf{w} \rightarrow \hat{\mathbf{w}}} = \sum_{k=1}^K \tau_{\mathbf{w} \rightarrow \hat{\mathbf{w}}}(k)$. Then, the PEP conditioned on the channel fading vector for a maximum-likelihood receiver is given as [31]

$$\begin{aligned} \Pr\{\mathbf{w} \rightarrow \hat{\mathbf{w}}|\mathbf{h}\} &= Q\left(\sqrt{\frac{\|\text{diag}(\mathbf{h}) \sum_{j=1}^J (\mathbf{x}_j - \hat{\mathbf{x}}_j)\|^2}{2N_0}}\right) \\ &= Q\left(\sqrt{\frac{\sum_{k=1}^K h_k^2 \tau_{\mathbf{w} \rightarrow \hat{\mathbf{w}}}(k)}{2N_0}}\right), \end{aligned} \quad (10)$$

where $Q(\cdot)$ is the Gaussian Q -function i.e., $Q(x) = (2\pi)^{-1/2} \int_x^{+\infty} e^{-t^2/2} dt$. By applying the Chernoff bound to (10), i.e., $Q(x) \leq e^{-\frac{x^2}{2}}$ [42], we obtain

$$\Pr\{\mathbf{w} \rightarrow \hat{\mathbf{w}}|\mathbf{h}\} \leq \prod_{k=1}^K \exp\left(-\frac{h_k^2 \tau_{\mathbf{w} \rightarrow \hat{\mathbf{w}}}(k)}{4N_0}\right). \quad (11)$$

To derive the PEP $\Pr\{\mathbf{w} \rightarrow \hat{\mathbf{w}}\}$, we take expectation with respect to \mathbf{h} on both sides of (11). In downlink Rician channels, the distribution of h_k^2 relates to the non-central chi-square distribution with its moment generating function (MGF) given by [43]

$$M_{|h_k|^2}(s) = \frac{1 + \kappa}{1 + \kappa + s} \exp\left(-\frac{\kappa s}{1 + \kappa + s}\right). \quad (12)$$

Note that the MGF of a random variable Λ is computed as $\mathbb{E}[e^{s\Lambda}] = M_\Lambda(s)$. Hence, taking expectation with respect to \mathbf{h} on both sides of (11) and applying (12), we obtain

$$\Pr\{\mathbf{w} \rightarrow \hat{\mathbf{w}}\} \leq \prod_{k=1}^K \left\{ \frac{1 + \kappa}{1 + \kappa + \frac{\tau_{\mathbf{w} \rightarrow \hat{\mathbf{w}}}(k)}{4N_0}} \exp\left(\frac{-\kappa \frac{\tau_{\mathbf{w} \rightarrow \hat{\mathbf{w}}}(k)}{4N_0}}{1 + \kappa + \frac{\tau_{\mathbf{w} \rightarrow \hat{\mathbf{w}}}(k)}{4N_0}}\right) \right\}, \quad (13)$$

which can be written in the form

$$\Pr\{\mathbf{w} \rightarrow \hat{\mathbf{w}}\} \leq \exp\left(-\frac{d_{\mathbf{w} \rightarrow \hat{\mathbf{w}}}^2}{4N_0}\right), \quad (14)$$

with

$$\begin{aligned} d_{\mathbf{w} \rightarrow \hat{\mathbf{w}}}^2 &= \sum_{k=1}^K \left\{ \underbrace{\frac{\kappa \tau_{\mathbf{w} \rightarrow \hat{\mathbf{w}}}(k)}{1 + \kappa + \frac{\tau_{\mathbf{w} \rightarrow \hat{\mathbf{w}}}(k)}{4N_0}}}_{d_{1, \mathbf{w} \rightarrow \hat{\mathbf{w}}}^2(k)} \right. \\ &\quad \left. + \underbrace{4N_0 \ln\left(1 + \frac{\tau_{\mathbf{w} \rightarrow \hat{\mathbf{w}}}(k)}{4N_0(1 + \kappa)}\right)}_{d_{2, \mathbf{w} \rightarrow \hat{\mathbf{w}}}^2(k)} \right\}. \end{aligned} \quad (15)$$

We next examine some special cases of (14) at sufficiently high SNR values.

1). For $(1 + \kappa) \gg \frac{\tau_{\mathbf{w} \rightarrow \hat{\mathbf{w}}}(k)}{4N_0}$, we have

$$d_{1, \mathbf{w} \rightarrow \hat{\mathbf{w}}}^2(k) = \frac{\kappa \tau_{\mathbf{w} \rightarrow \hat{\mathbf{w}}}(k)}{\kappa + 1}, \quad d_{2, \mathbf{w} \rightarrow \hat{\mathbf{w}}}^2(k) = 0, \quad (16)$$

and thus $d_{\mathbf{w} \rightarrow \hat{\mathbf{w}}}^2 = \frac{\kappa \delta_{\mathbf{w} \rightarrow \hat{\mathbf{w}}}}{1 + \kappa}$. In this special case, (14) reduces to

$$\Pr\{\mathbf{w} \rightarrow \hat{\mathbf{w}}\} \leq \exp\left(-\frac{\kappa \delta_{\mathbf{w} \rightarrow \hat{\mathbf{w}}}}{4(1 + \kappa)N_0}\right). \quad (17)$$

2). In the case when $(1 + \kappa) \ll \frac{\tau_{\mathbf{w} \rightarrow \hat{\mathbf{w}}}(k)}{4N_0}$, we have

$$d_{1, \mathbf{w} \rightarrow \hat{\mathbf{w}}}^2(k) = 4N_0 \kappa, \quad d_{2, \mathbf{w} \rightarrow \hat{\mathbf{w}}}^2(k) = 4N_0 \ln\left(-\frac{\tau_{\mathbf{w} \rightarrow \hat{\mathbf{w}}}(k)}{4N_0(1 + \kappa)}\right), \quad (18)$$

and thus $d_{\mathbf{w} \rightarrow \hat{\mathbf{w}}}^2$ is the sum of the logarithms of the element-wise distance. To proceed, let us define

$$\begin{aligned} D(\mathbf{w} \rightarrow \hat{\mathbf{w}}) &\triangleq \{k : \tau_{\mathbf{w} \rightarrow \hat{\mathbf{w}}}(k) \neq 0, 1 \leq k \leq K\}, \\ G_d(\mathbf{w} \rightarrow \hat{\mathbf{w}}) &\triangleq \sum_{k=1}^K \text{Ind}(\tau_{\mathbf{w} \rightarrow \hat{\mathbf{w}}}(k)), \end{aligned} \quad (19)$$

where $\text{Ind}(x)$ takes the value of one if x is nonzero and zero otherwise. Clearly, $G_d(\mathbf{w} \rightarrow \hat{\mathbf{w}})$ gives the cardinality of set $D(\mathbf{w} \rightarrow \hat{\mathbf{w}})$. Substituting (18) and (15) into (14), we obtain the PEP for this special case as

$$\Pr\{\mathbf{w} \rightarrow \hat{\mathbf{w}}\} \leq \prod_{k \in D(\mathbf{w} \rightarrow \hat{\mathbf{w}})} \left(\frac{\tau_{\mathbf{w} \rightarrow \hat{\mathbf{w}}}(k)}{4N_0(1 + \kappa)}\right)^{-1} \exp(-\kappa). \quad (20)$$

Note that one can approximate the right-hand side of (20) as

$$\Pr\{\mathbf{w} \rightarrow \hat{\mathbf{w}}\} \leq G_c(\mathbf{w} \rightarrow \hat{\mathbf{w}}) \left(\frac{1}{4N_0(1 + \kappa)}\right)^{-G_d(\mathbf{w} \rightarrow \hat{\mathbf{w}})}, \quad (21)$$

where

$$G_c(\mathbf{w} \rightarrow \hat{\mathbf{w}}) = \prod_{k \in D_k(\mathbf{w} \rightarrow \hat{\mathbf{w}})} \tau_{\mathbf{w} \rightarrow \hat{\mathbf{w}}}(k)^{-1} \exp(-\kappa). \quad (22)$$

Let $G_d \triangleq \min_{\mathbf{w} \neq \hat{\mathbf{w}}} G_d(\mathbf{w} \rightarrow \hat{\mathbf{w}})$ and $G_c \triangleq \min_{\mathbf{w} \neq \hat{\mathbf{w}}} G_c(\mathbf{w} \rightarrow \hat{\mathbf{w}})$, where G_d and G_c are the so-called diversity gain and coding gain [41]. The coding advantage G_c is an approximate measure of the gain operating with the same diversity advantage. Note that the PEP for AWGN and Rayleigh fading channels can also be obtained by respectively letting $\kappa \rightarrow \infty$ in (17) and $\kappa = 0$ in (21).

B. Design criteria of multi-dimensional codebook

Define $n_e(\mathbf{w}, \hat{\mathbf{w}})$ as the erroneous bits when $\hat{\mathbf{w}}$ is decoded at receiver, the union bound of average bit error rate (ABER) for SCMA systems is given below:

$$P_b \leq \frac{1}{M^J \cdot J \log_2(M)} \cdot \sum_{\mathbf{w}} \sum_{\hat{\mathbf{w}} \neq \mathbf{w}} n_e(\mathbf{w}, \hat{\mathbf{w}}) \cdot \Pr\{\mathbf{w} \rightarrow \hat{\mathbf{w}}\}. \quad (23)$$

At large SNRs, as the ABER is mainly dominated by the largest value of PEP in (14), we assert that improving the minimum distance of $d_{\mathbf{w} \rightarrow \hat{\mathbf{w}}}^2$ among all pairs will lead to lower ABER. Hence, we formulate our codebook design of the SCMA system with structure $\mathcal{S}(\mathcal{V}, \mathcal{G}; J, M, N, K)$, $\mathcal{V} := [\mathbf{V}_j]_{j=1}^J$ and $\mathcal{G} := [g_j]_{j=1}^J$ in downlink Rician fading channels as

$$\mathcal{V}^*, \mathcal{G}^* = \arg \max_{\mathcal{V}, \mathcal{G}} \Delta_{\min}, \quad (24)$$

where Δ_{\min} denotes the minimum distance in Rician channels and is obtained by calculating $M^J (M^J - 1)/2$ mutual distances between M^J superimposed codewords, i.e.,

$$\Delta_{\min} \triangleq \min \{d_{\mathbf{w} \rightarrow \hat{\mathbf{w}}}^2 | \forall \mathbf{w}, \hat{\mathbf{w}} \in \Phi_{M^J}, \mathbf{w} \neq \hat{\mathbf{w}}\}. \quad (25)$$

Remark 1: For $\kappa \rightarrow 0$, from (21) we observe the PEP decays with the slope of $(1/(\kappa + 1) N_0)^{-G_d}$ and the system achieves the diversity order of G_d . The ABER is mainly dominated by the single error event that all the codewords are detected correctly except for a codeword of only one layer. In other words, for the pairs \mathbf{w} and $\hat{\mathbf{w}}$ such that $G_d(\mathbf{w} \rightarrow \hat{\mathbf{w}}) = G_d$, the term $\prod_{k \in D_k(\mathbf{w} \rightarrow \hat{\mathbf{w}})} \tau_{\mathbf{w} \rightarrow \hat{\mathbf{w}}}(k)^{-1}$ in (22) equals to the product distance of an MC. Note that let $\kappa = 0$ (Rayleigh fading channel) in (24), an equivalent expression can also be obtained.

Remark 2: For $\kappa \rightarrow \infty$ (Gaussian channel), we have $\kappa/(1 + \kappa) \approx 1$. Then, based on (17) and (23), we know that the ABER is dominated by the MED between \mathbf{w} and $\hat{\mathbf{w}}$ in Φ_{M^J} , which corresponding to the multiple error events that all the errors occurred with multiple layers. Therefore, an important codebook design criteria in this case is to maximize the MED of the superimposed codewords, which has been widely employed for SCMA systems operating in the AWGN channel [27], [29], [33]. Similarly, the MED can also be obtained by letting $\kappa \rightarrow \infty$ in (24).

IV. PROPOSED LOW-PROJECTION CODEBOOK DESIGN

This section introduces our proposed LPCBs that enable low complexity detection with the proposed minimum distance metric. The main design steps are: generate a one-dimensional LPGAM vector, permute LPGAM to obtain an N -dimensional MC, optimize the constellation operators, and optimize the bit-to-symbol labeling. To enhance the shaping gain, we propose to jointly optimize the MC and constellation operators.

A. Design of one-dimensional LPGAM

Denote $\mathcal{A}_{M,T}$ as a length- M one-dimensional LPGAM vector with T distinct elements, i.e., $M - T$ constellation points are overlapped. To obtain $\mathcal{A}_{M,T}$, we first construct a constellation \mathcal{A}_T with T points, then repeat $M - T$ points in \mathcal{A}_T by following certain rules. The selection of the \mathcal{A}_T is of vital importance to downlink SCMA codebook design. In this

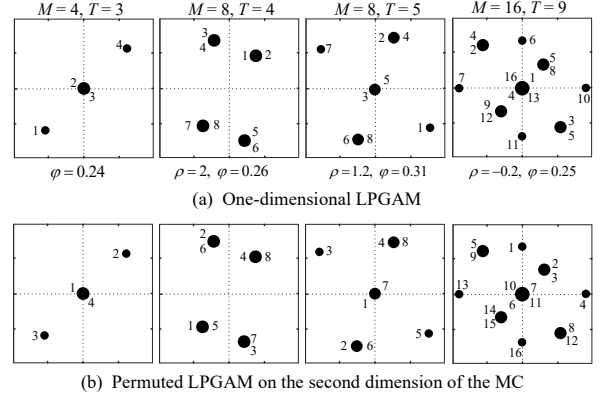


Fig. 2: Examples of $\mathcal{A}_{M,T}$ and $\pi_2(\mathcal{A}_{M,T})$.

paper, we employ GAM to design the \mathcal{A}_T due to the attractive features of enhanced mutual information, distance and PAPR performance [39]. The n th constellation point of GAM with N_p points can be generated according to $x_n = r_n e^{i2\pi\omega n}$, where $r_n = c_{\text{norm}} \sqrt{n}$, $c_{\text{norm}} = \sqrt{\frac{2P}{N_p+1}}$, P is the power constraint and $\omega = \frac{1-\sqrt{5}}{2}$ is the golden angle in radians. The design procedure of $\mathcal{A}_{M,T}$ is specified as follows:

1) *Generate \mathcal{A}_T :* Generate the GAM points according to $x_n = c_{\text{norm}} \sqrt{n + \rho} \cdot e^{i2\pi(\varphi + \omega)n}$, where φ is an arbitrary angle and ρ is the amplitude factor. Note that in the proposed LPGAM, we have two additional degrees of freedom for enhanced codebook design, i.e., ρ and φ . Such a constellation is referred to as (ρ, φ) -GAM. The construction steps of \mathcal{A}_T are as follows: 1) For even value of T , generate $N_p = \frac{T}{2}$ (ρ, φ) -GAM points, denoted by $\mathcal{A}_T^{(m)}$, $m = 1, 2, \dots, \frac{T}{2}$. The remaining $\frac{T}{2}$ points are obtained by symmetry: $\mathcal{A}_T^{(m+\frac{T}{2})} = -\mathcal{A}_T^{(m)}$ for $m = 1, 2, \dots, \frac{T}{2}$; 2) For odd value of T , generate $N_p = \frac{T-1}{2}$ (ρ, φ) -GAM points. Similarly, the other $\frac{T-1}{2}$ points are obtained by symmetry. Finally, the zero point in the complex domain is added to \mathcal{A}_T .

2) *Obtain $\mathcal{A}_{M,T}$ based on \mathcal{A}_T :* After generating the \mathcal{A}_T based on GAM, the next problem is how to allocate \mathcal{A}_T with overlapped signal points to a length- M vector. To proceed, let us define $\mathcal{P}_{M,T} = \{p_1, p_2, \dots, p_L\}$ and $\mathcal{T}_{M,T} = \{t_1, t_2, \dots, t_L\}$ as the overlapped signal set and corresponding projected numbers, respectively, where $p_l \in \mathcal{A}_T$, $1 \leq l \leq L$ and $\sum_{l=1}^L t_l = M - T$. Namely, the constellation point p_l is overlap t_l times in $\mathcal{A}_{M,T}$. The following rules are adopted to determine \mathcal{P} and \mathcal{T} :

- The overlapping number for a particular constellation point, i.e., t_l , should be as small as possible, such that the constructed MC has a good distance property.
- The constellation points with lower energy in \mathcal{A}_T are preferentially added to $\mathcal{P}_{M,T}$, such that the constellation \mathcal{A}_M has a small average energy.
- \mathcal{P} and \mathcal{T} should exhibit certain symmetry, such that the obtained \mathcal{A}_M is also symmetrical and with a zero mean.

Next, we give an example of the constructed LPGAM in Fig. 2(a). One can see that there are $M - T$ constellation points

overlapped in LPGAM, where the overlapped constellation set, i.e., $\mathcal{P}_{M,T}$ and $\mathcal{T}_{M,T}$ are predefined according to the above rules. Note that the LPGAM of $M = 4$, $T = 3$ is a special case, in which the constellation is only determined by φ .

B. Construction of the N -dimension MC

After obtaining the one-dimensional constellation $\mathcal{A}_{M,T}$, the remaining $N - 1$ dimensions may be obtained by the repetition of $\mathcal{A}_{M,T}$. To obtain a higher gain, permutation is further applied to $\mathcal{A}_{M,T}$. Let $\pi_n : [1, 2, \dots, M]^T \rightarrow [\pi_{n,1}, \pi_{n,2}, \dots, \pi_{n,M}]^T$ denote the permutation mapping of the n th dimension, where $\pi_{n,m}$, $1 \leq \pi_{n,m} \leq M$ denotes the permutation index, and for $m \neq l$, $\pi_{n,m} \neq \pi_{n,l}$. Namely, the $\pi_{n,m}$ th constellation point in $\mathcal{A}_{M,T}$ is permuted to the m th position of $\pi_n(\mathcal{A}_{M,T})$ at n th dimension. Then the N -dimensional constellation $\mathcal{C}_{MC} = [\bar{\mathbf{c}}_1^T, \bar{\mathbf{c}}_2^T, \dots, \bar{\mathbf{c}}_M^T]^T$ can be obtained as

$$\mathcal{C}_{MC} = [\pi_1(\mathcal{A}_{M,T}), \pi_2(\mathcal{A}_{M,T}), \dots, \pi_N(\mathcal{A}_{M,T})]^T. \quad (26)$$

To proceed, we further define the N -dimensional Cartesian product over the one-dimensional \mathcal{A}_T as

$$\begin{aligned} \mathcal{A}_T^N &= \underbrace{\mathcal{A}_T \times \mathcal{A}_T \times \dots \times \mathcal{A}_T}_N \\ &\triangleq \{(a_1, a_2, \dots, a_N) | \forall a_i \in \mathcal{A}_T, \forall i \in \{1, 2, \dots, N\}\}, \end{aligned} \quad (27)$$

where “ \times ” denotes the Cartesian product. By transforming every element in \mathcal{A}_T^N into a column vector, we obtain an N -dimensional matrix $\mathbf{A} \in \mathbb{C}^{N \times T^N}$. For simplicity, we denote the above Cartesian mapping as $f_{\mathbf{A}} : \mathcal{A}_T^N \rightarrow \mathbf{A}$. Then, we introduce the following lemma:

Lemma 1: To construct an N -dimensional \mathcal{C}_{MC} , the LP number should satisfy $\lceil \sqrt[N]{M} \rceil \leq T \leq M$. For the case of $T = \sqrt[N]{M} \in \mathbb{Z}$, the permutation π_n , $n = 1, 2, \dots, N$ are given by the mapping $f_{\mathbf{A}}$.

Proof: Refer to Appendix A.

For the other values of T and M , we first fix the constellation at the first dimension with a randomly chosen permutation. Accordingly, for the second dimension, there will be a total of $T = M!$ pairing options. Consequently, there are $T = (M!)^{N-1}$ different choices of the permutations. The MC constrained PEP can be employed to aid the design of permutation metric. To this end, we further define $d_{\min,t}^{\mathcal{C}_{MC}}$, $t = 1, 2, \dots, T$ as the minimum effective distance from the $M(M-1)/2$ mutual codeword distances arising from \mathcal{C}_{MC} . Based on the results in (14) and (15), we have

$$\begin{aligned} d_{\min,t}^{\mathcal{C}_{MC}} &= \arg \min_{1 \leq i < l \leq M} \sum_{n=1}^N \frac{\kappa |c_{n,i}^{(t)} - c_{n,l}^{(t)}|^2}{1 + \kappa + \frac{|c_{n,i}^{(t)} - c_{n,l}^{(t)}|^2}{4N_0}} \\ &\quad + 4N_0 \ln \left(1 + \frac{|c_{n,i}^{(t)} - c_{n,l}^{(t)}|^2}{4N_0(1 + \kappa)} \right), \end{aligned} \quad (28)$$

where $c_{n,i}^{(t)}$ denotes the i th symbol at the n th entry of \mathcal{C}_{MC} . Hence, the permutation should be chosen to maximise (28), i.e.,

$$\mathcal{C}_{MC}^* = \arg \max_{t=1,2,\dots,T} d_{\min,t}^{\mathcal{C}_{MC}}. \quad (29)$$

Lemma 2: By substituting $\kappa \rightarrow \infty$ (AWGN) and $\kappa = 0$ (Rayleigh fading) in (30), the equivalent distance metrics $d_{\min,t}^{\mathcal{C}_{MC}}$ are obtained as

$$d_{E,\min,t}^{\mathcal{C}_{MC}} = \arg \min_{i \neq l} \| \mathbf{c}_i^{(t)} - \mathbf{c}_l^{(t)} \|^2, \quad (30)$$

and

$$d_{P,\min,t}^{\mathcal{C}_{MC}} = \arg \min_{i \neq l} \prod_{n \in \rho(\mathbf{c}_i, \mathbf{c}_l)} |c_{n,i}^{(t)} - c_{n,l}^{(t)}|^2, \quad (31)$$

respectively, where $\rho(\mathbf{c}_i, \mathbf{c}_j)$ denotes the set of indices in which $c_{n,i} \neq c_{n,j}$. Clearly, the MED and MPD are the corresponding permutation criteria for AWGN and Rayleigh fading channels, respectively.

For small constellation size, e.g., $M \leq 8$ and $N \leq 2$, one can find the optimal permutation by exhaustive search with reasonable computational complexity. However, for large constellation size of \mathcal{C}_{MC} , it becomes intractable due to the huge number of permutation pairs. To overcome such a difficulty, the binary switching algorithm (BSA) [44] can be modified to find the sub-optimal permutation pattern. Fig. 2(b) shows the permuted constellation corresponding to the LPGAM in Fig. 2(a) for a 2-dimensional \mathcal{C}_{MC} . Taking \mathcal{C}_{MC} with $N = 2$, $M = 4$, $T = 3$ as an example, the second and third points are overlapped at the first dimension; however, they are separated at the second dimension with the permutation.

C. Sparse codebook construction

After the design of the \mathcal{C}_{MC} , phase rotations are applied to generate multiple sparse codebooks. In addition, aiming at increasing the power diversity between users and improving the minimum distance properties of the superimposed codewords, we introduce energy scaling to each codebook dimension [29]. Specifically, the j th user's codebook with non-zero elements is generated by $\mathcal{C}_j = \mathbf{E}_j \mathbf{R}_j \mathcal{C}_{MC}$, where \mathbf{R}_j and \mathbf{E}_j denote the phase rotation matrix and power scaling matrix for the j th user, respectively. Note that the phase rotation matrix and power scaling matrix can be combined together to form a constellation operator matrix, denoted as $\Delta_j = \mathbf{E}_j \mathbf{R}_j$. For example, for a 2-dimensional \mathcal{C}_{MC} , \mathbf{E}_j and \mathbf{R}_j are given as

$$\mathbf{E}_j = \begin{bmatrix} E_1 & 0 \\ 0 & E_2 \end{bmatrix}, \mathbf{R}_j = \begin{bmatrix} e^{j\theta_1} & 0 \\ 0 & e^{j\theta_2} \end{bmatrix}, \Delta_j = \begin{bmatrix} z_1 & 0 \\ 0 & z_2 \end{bmatrix}, \quad (32)$$

where $z_i = E_i e^{j\theta_i}$, $\forall E_i > 0, 1 \leq i \leq N$. Based on \mathbf{V}_j which has been introduced in Section II, the j th user's codebook is generated by $\mathcal{X}_j = \mathbf{V}_j \Delta_j \mathcal{C}_{MC}$. We further combine the constellation operation matrix Δ_j and mapping matrix \mathbf{V}_j together, i.e., $\mathbf{z}_{N \times J}^j = \mathbf{V}_j \Delta_j \mathbf{I}_K$, where \mathbf{I}_K denotes a column vector of K 's. Hence, J codebooks can be represented by the signature matrix $\mathbf{Z}_{N \times J} = [\mathbf{z}_{N \times J}^1, \dots, \mathbf{z}_{N \times J}^J]$.

Owing to the sparsity of the factor graph matrix, the number of users superimposed on one resource node is d_f which is less than the number of users. Therefore, d_f distinct rotation angles and scaling factors of each dimension should be optimized to distinguish the superimposed codewords. Different from the Latin rectangular construction, we consider the signature

matrix $\mathbf{Z}_{K \times J}$ for (4×6) and (5×10) SCMA systems [29] as follows:

$$\mathbf{Z}_{4 \times 6} = \begin{bmatrix} 0 & z_1 & z_2 & 0 & z_3 & 0 \\ z_1 & 0 & z_2 & 0 & 0 & z_3 \\ 0 & z_3 & 0 & z_2 & 0 & z_1 \\ z_3 & 0 & 0 & z_2 & z_1 & 0 \end{bmatrix}, \quad (33)$$

$$\mathbf{Z}_{5 \times 10} = \begin{bmatrix} z_1 & z_2 & z_3 & z_4 & 0 & 0 & 0 & 0 & 0 & 0 \\ z_4 & 0 & 0 & 0 & z_1 & z_2 & z_3 & 0 & 0 & 0 \\ 0 & z_3 & 0 & 0 & z_4 & 0 & 0 & z_1 & z_2 & 0 \\ 0 & 0 & z_2 & 0 & 0 & z_3 & 0 & z_4 & 0 & z_1 \\ 0 & 0 & 0 & z_1 & 0 & 0 & z_2 & 0 & z_3 & z_4 \end{bmatrix}. \quad (34)$$

Observing the power diversity, row-wise or column wise, with $|z_i| \neq |z_j|, \forall 1 \leq i < j \leq d_f$, may help improve the Δ_{\min} . Power imbalance among different users is also introduced into $\mathbf{Z}_{4 \times 6}$ and $\mathbf{Z}_{5 \times 10}$ by $|z_1| + |z_3| \neq 2|z_2|$ and $|z_1| + |z_4| \neq |z_2| + |z_3|$, respectively. The phase rotation angles $\boldsymbol{\theta} = [\theta_1, \theta_2, \dots, \theta_{d_f}]^T$ and the energy factors $\mathbf{E} = [E_1, E_2, \dots, E_{d_f}]^T$ are the parameters to be optimized, where the degree of freedom for $\boldsymbol{\theta}$ and \mathbf{E} is $d_f - 1$. The other two parameters to be jointly optimized are the ρ and φ of the GAM constellation. Hence, the number of parameters to be optimized for the proposed codebooks is $2(d_f - 1) + 1$ and $2(d_f - 1) + 2$ for $M = 4$ and $M > 4$, respectively.

Let $\mathcal{X}_{\lambda, M, T}$ be the M -ary codebook set with T projected numbers to be optimized for the SCMA system with the overloading $\lambda \in \{150\%, 200\%\}$. As discussed in Subsection III-B, the design goal is to maximize the minimum distance metric Δ_{\min} which is defined in (38). Hence, based on the proposed multi-dimensional codebook construction scheme, the codebook design is formulated as

$$\begin{aligned} & \max_{\mathbf{E}, \boldsymbol{\theta}, \rho, \varphi} \Delta_{\min}(\mathcal{X}_{\lambda, M, T}) \\ & \text{Subject to} \quad \sum_{i=1}^{d_f} E_i = \frac{MJ}{K}, E_i > 0, \\ & \quad 0 \leq \theta_i \leq \pi, \\ & \quad -1 < \rho \leq T, \\ & \quad 0 \leq \varphi \leq \pi/2. \\ & \quad \forall i = 1, 2, \dots, d_f. \end{aligned} \quad (35)$$

Unfortunately, it is quite difficult, if not impossible, to directly solve the optimization problem in (35) due to the non-convex and high computation complexity of the objective function. For the $M = 4$ and $J = 6$ SCMA system, the computational complexity of $\Delta_{\min}(\mathcal{X}_{\lambda, M, T})$ is moderate. However, as the increase of K, J and M , it brings overwhelming computational complexity to calculate $\Delta_{\min}(\mathcal{X}_{\lambda, M, T})$. Hence, for a highly overloaded SCMA system or high rate ($M \geq 8$) codebooks, we transform (35) to a feasible problem with affordable complexity by considering the distinct features of LPCBs.

1) *The case of $T = \sqrt[d_f]{M}$:* Let $\mathcal{S}_{\text{sum}}^k$ denote the superimposed constellation at the k th resource node after removing the overlapped constellation in \mathcal{C}_{MC} . Namely, all constellation points in $\mathcal{S}_{\text{sum}}^k$ are unique and $|\mathcal{S}_{\text{sum}}^k| = T^{d_f}$. According to (33) and (34), $\mathcal{S}_{\text{sum}}^k$ can be obtained by $\mathcal{S}_{\text{sum}}^{(k)} = \{z_1 a_1 + z_2 a_2 + \dots + z_{d_f} a_{d_f} | \forall a_i \in \mathcal{A}_T, i = 1, 2, \dots, d_f\}$. For simplicity, and since each resource node has the same superimposed constellation, the superscript (k) is omitted. Then, we introduce the following Lemma:

Lemma 3: For the $\mathcal{X}_{\lambda, M, T}$ where $T = \sqrt[d_f]{M}$, maximizing $\Delta_{\min}(\mathcal{X}_{\lambda, M, T})$ is equivalent to maximizing the MED of \mathcal{S}_{sum} , which is defined as

$$\text{MED}(\mathcal{S}_{\text{sum}}) \triangleq \min \{|s_m - s_n|^2, | \forall s_n, s_m \in \mathcal{S}_{\text{sum}}, \forall m, n \in Z_{T^{d_f}}, m \neq n \}. \quad (36)$$

Proof: Refer to Appendix B.

Since T^{d_f} is relatively small, the complexity of calculating $\text{MED}(\mathcal{S}_{\text{sum}})$ is negligible.

2) *For the case when $T > \sqrt[d_f]{M}$:* We propose to maximize the lower bound of $\Delta_{\min}(\mathcal{X}_{\lambda, M, T})$. To proceed, let us first define

$$d_{1, \min}^{\mathcal{X}_{\lambda, M, T}} \triangleq \min \left\{ \sum_{k=1}^K d_{1, \mathbf{w} \rightarrow \hat{\mathbf{w}}}^2 | \forall \mathbf{w}, \hat{\mathbf{w}} \in \Phi_{MJ}, \mathbf{w} \neq \hat{\mathbf{w}} \right\}, \quad (37)$$

and

$$\begin{aligned} d_{2, \min}^{\mathcal{X}_{\lambda, M, T}} & \triangleq \min \left\{ \sum_{k=1}^K d_{2, \mathbf{w} \rightarrow \hat{\mathbf{w}}}^2 | \forall \mathbf{w}, \hat{\mathbf{w}} \in \Phi_{MJ}, \mathbf{w} \neq \hat{\mathbf{w}} \right\}, \\ & \stackrel{(i)}{=} \min_{1 \leq j \leq J} \left\{ \sum_{k=1}^K 4N_0 \ln \left(1 + \frac{|x_{j,i,k} - x_{j,l,k}|^2}{4N_0(1+\kappa)} \right) \right. \\ & \quad \left. | \forall x_{j,i,k}, x_{j,l,k} \in \mathcal{X}_j, \forall i, l \in Z_M, i \neq l \right\}, \end{aligned} \quad (38)$$

where $d_{1, \mathbf{w} \rightarrow \hat{\mathbf{w}}}^2$ and $d_{2, \mathbf{w} \rightarrow \hat{\mathbf{w}}}^2$ are given in (15). (i) holds true since the minimum distance metric between superimposed codewords is achieved when the single error event occurs. Obviously, for the codebook $\mathcal{X}_{\lambda, M, T}$,

$$\Delta_{\text{LB}}(\mathcal{X}_{\lambda, M, T}) \triangleq d_{1, \min}^{\mathcal{X}_{\lambda, M, T}} + d_{2, \min}^{\mathcal{X}_{\lambda, M, T}} \quad (39)$$

is a lower bound of $\Delta_{\min}(\mathcal{X}_{\lambda, M, T})$. Note that $\Delta_{\text{LB}}(\mathcal{X}_{\lambda, M, T})$ and $\Delta_{\min}(\mathcal{X}_{\lambda, M, T})$ may not achieve the minimum value at the same solution, however, the value of $\Delta_{\min}(\mathcal{X}_{\lambda, M, T})$ can still be improved by maximizing $\Delta_{\text{LB}}(\mathcal{X}_{\lambda, M, T})$. Moreover, upon taking into account of *Remark 1* and *Remark 2* in Subsection III-B, one can see that improving the $d_{1, \min}^{\mathcal{X}_{\lambda, M, T}}$ and $d_{2, \min}^{\mathcal{X}_{\lambda, M, T}}$ can also reduce the probability of multiple and single error events, respectively. In fact, for large or small value of κ , $\Delta_{\text{LB}}(\mathcal{X}_{\lambda, M, T})$ is very tight. Hence, instead of directly maximizing $\Delta_{\min}(\mathcal{X}_{\lambda, M, T})$, we propose to maximize its lower bound $\Delta_{\text{LB}}(\mathcal{X}_{\lambda, M, T})$, where the computational complexity of $d_{2, \min}^{\mathcal{X}_{\lambda, M, T}}$ is negligible since it only involves the calculation of \mathcal{X}_j .

For the sparse codebook optimization problem, it is designed with the highly non-linear objective function and linear constraints. Such problem can be efficiently solved with an optimization solver, e.g. MATLAB Global Optimization toolbox. In particular, we employ the interior-point method in the *fmincon* solver to address the problem (35). The maximum iteration number for $\lambda = 150\%$ and $\lambda = 200\%$ SCMA systems are 30 and 25, respectively. Although the complexity of $\Delta_{\text{LB}}(\mathcal{X}_{\lambda, M, T})$ has been significantly reduced, the calculation of $d_{1, \min}^{\mathcal{X}_{\lambda, M, T}}$ is still a challenging problem for $M \geq 16$ or $d_f = 4$. To solve this problem, a sub-optimal Monte Carlo search method is adopted. The distance metric $d_{1, \min}^{\mathcal{X}_{\lambda, M, T}}$ is first calculated between Q elements, which is randomly selected from the superimposed codewords Φ . Then, the above process

Algorithm 1 Modified BSA for SCMA codebook.

Input: Optimized codebook \mathcal{X}_j
Output: A locally optimum bit-to-symbol mapping \mathbf{z} for \mathcal{X}_j

- 1: **Initialize:** Randomly choose an index vector \mathbf{z} for codebook \mathcal{X}_j and sort \mathcal{X}_j out based on the random index vector, and set $\mathbf{z}^* = \mathbf{z}$
- 2: **for** $I = 1 : I_{\max}$ **do**
- 3: Obtain $\Xi(\mathbf{x}_{j,i}), i = 1, 2, \dots, M$ and Π_{ini} by updating the cost of $\mathcal{X}_j(\mathbf{z}^*)$ using (40)
- 4: Sort $\Xi(\mathbf{x}_{j,i})$ in decreasing order and obtain the new index vector \mathbf{z}
- 5: **for** $i = 1 : M$ **do**
- 6: **for** $l = 1 : M$ **do**
- 7: **if** $\mathbf{z}(i) = l$ **then** next l
- 8: Switch the $\mathbf{z}(i)$ -th codeword with l -th codeword and update the index vector $\bar{\mathbf{z}}$
- 9: Calculate the total cost Π_{sw} using (40)
- 10: **if** $\Pi_{\text{sw}} \leq \Pi_{\text{ini}}$ **then**
- 11: Retain the switch, and update \mathbf{z}^* and Π_{ini} with $\bar{\mathbf{z}}$ and Π_{sw} , respectively
- 12: **else**
- 13: Switch back the two symbols
- 14: **end if**
- 15: **end for**
- 16: **end for**
- 17: **end for**

is repeated with t_{\max} times to estimate the $d_{1,\min}^{\mathcal{X}_\lambda, M, T}$.

D. Labeling design for each user

For each sparse codebook \mathcal{X}_j , the corresponding bit-to-symbol mapping, i.e., bit labeling, needs to be optimized. Similar to the case of permutation, the labeling rules should be designed to minimize the MC constrained ABER. Under Rician fading channels, the labeling metric is given as

$$\Pi(\xi_t) = \sum_{i=1}^{M-1} \underbrace{\sum_{l=1, l \neq i}^M N_{i,l}(\xi_j) \exp\left(\frac{-d_{t,i,l}}{4N_0}\right)}_{\Xi(\mathbf{x}_{j,i})}, \quad (40)$$

where $N_{i,l}(\xi_t)$ denotes the number of different labelling bits between $\mathbf{x}_{j,i}$ and $\mathbf{x}_{j,l}$ based on the considered labelling rule ξ_t , $\Xi(\mathbf{x}_{j,i})$ denotes the cost for the i th codeword of \mathcal{X}_j , and $d_{t,i,l}$ is given as

$$d_{t,i,l} = \sum_{k=1}^K \left\{ \frac{\kappa |x_{i,k}^{(t)} - x_{l,k}^{(t)}|^2}{1 + \kappa + \frac{|x_{i,k}^{(t)} - x_{l,k}^{(t)}|^2}{4N_0}} + 4N_0 \ln \left(1 + \frac{|x_{i,k}^{(t)} - x_{l,k}^{(t)}|^2}{4N_0(1 + \kappa)} \right) \right\}, \quad (41)$$

where $x_{i,k}^{(t)}$ represents the element of \mathbf{x}_i at the k th entry for the labeling rule ξ_t .

Lemma 4: Obviously, let $\kappa \rightarrow \infty$ and $\kappa = 0$ in (41), we

Algorithm 2 Construction of LPCBs.

Input: $J, K, \mathbf{V}_j, M, T, \kappa, N_0, \mathcal{P}_{M,T}$ and $\mathcal{T}_{M,T}$

- 1: **Initialize:** $E_i, \theta_i, i = 1, 2, \dots, d_f, \rho, \varphi$
- 2: **Step 1 :** For the given M and T , generate the MC $\mathcal{A}_{M,T}$ based on GAM according to $\mathcal{P}_{M,T}$ and $\mathcal{T}_{M,T}$.
- 3: **Step 2 :** Perform a permutation according to the criteria given in (28) to obtain the N -dimensional MC, i.e., \mathcal{C}_{MC} .
- 4: **Step 3 :** Generate the j th user's codebook by $\mathcal{X}_j = \mathbf{V}_j \Delta_j \mathcal{C}_{MC}$.
- 5: **Step 4 :** Jointly optimize the MC and Δ_j by maximizing $\text{MED}(\mathcal{S}_{\text{sum}})$ or $\Delta_{\text{LB}}(\mathcal{X}_{\lambda, M, T})$.
- 6: **Step 5 :** Perform the bit labeling with **Algorithm 1** for the optimized codebook \mathcal{X}_j^* , and use the labeling metric given in (40).

can also obtain the equivalent labeling metric

$$\Pi_A(\xi) = \sum_{i=1}^{M-1} \sum_{l=i+1}^M N_{i,l}(\xi) \exp\left(\frac{-\|\mathbf{x}_{j,i} - \mathbf{x}_{j,l}\|}{4N_0}\right), \quad (42)$$

and

$$\Pi_R(\xi) = \sum_{i=1}^{M-1} \sum_{l=i+1}^M \frac{N_{i,l}(\xi)}{\prod_{k' \in \rho(\mathbf{x}_{j,i}, \mathbf{x}_{j,l})} |x_{j,i,k'} - x_{j,l,k'}|^2}, \quad (43)$$

for AWGN and Rayleigh fading channels, respectively.

There are $T = M!$ labeling options for an M -ary constellation. Hence, for large modulation order M , the complexity of exhaustive search is prohibitively high. The BSA can be employed again to find the labeling solution with reasonable complexity. A modified BSA for SCMA codebooks is described in **Algorithm 1**. In the BSA based labeling design, we first randomly initialize the labelling bits to M codewords, and calculate the cost value $\Pi(\xi_j)$ based on (40). Then, starting from the first codeword, we calculate the individual cost $\Xi(\mathbf{x}_{j,i})$ for all codewords and sort them out in decreasing order. Next, the algorithm swaps codeword index with the highest individual cost with another to find a lower total cost. **Algorithm 1** can be performed several times with different initial conditions to prevent it from jumping into local optimum. **Algorithm 1** can significantly reduce the computation complexity of searching labelling pattern. For each M -ary codebook, the computation complexity of exhaustive search can be approximated by $\mathcal{O}(M!)$. In contrast, the complexity of **Algorithm 1** can be estimated as $\mathcal{O}(I_{\max} M^2)$. For example, the reduction in complexity levels reaches 79% and 99% when considering $M = 8$ and $M = 16$, respectively.

To sum up, we have proposed an efficient codebook design with LP numbers in the downlink Rician fading channel and the overall construction procedures are given in **Algorithm 2**.

V. NUMERICAL RESULTS

In this section, we conduct numerical evaluations of the proposed LPCBs for the (4×6) and (5×10) SCMA systems characterized in (4) and (5), respectively. These two systems lead to overloading factors of $\lambda = 150\%$ and $\lambda = 200\%$,

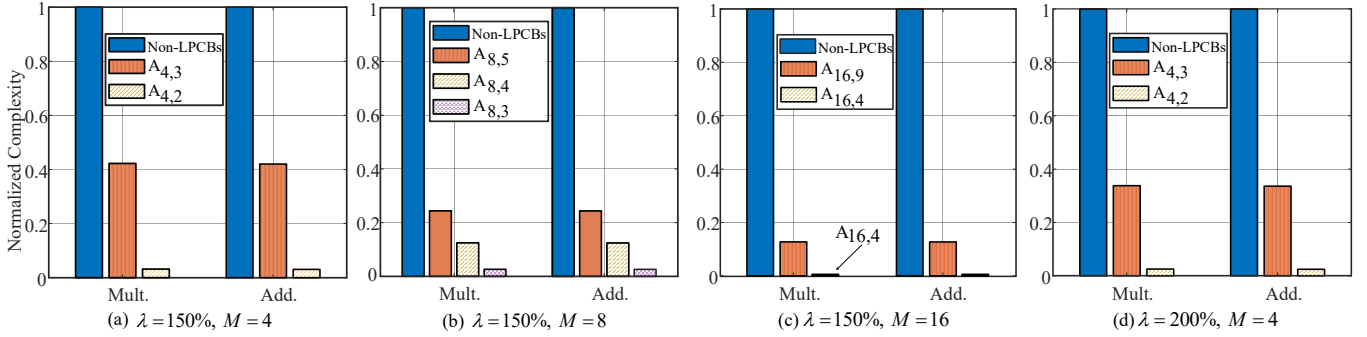


Fig. 3: Normalized complexity comparison between different codebooks.

respectively. Let $A_{M,T}$ denote the proposed LPCB of M -ary with T LP numbers. Since the proposed permutation, labeling and sparse codebook optimization criteria are applicable in the high E_b/N_0 regime, we consider $E_b/N_0 = 16$ dB, which is sufficiently large. In general, in an S-IoT networks with an LOS path, a large κ is assumed for the most scenarios [36]–[38]. Hence, we set $\kappa = 20$ for the optimization of the proposed LPCBs. Moreover, considering the trade-off between the computation complexity and accuracy, we set $Q = 10000$ and $t_{\max} = 20$ for the cases of $M \geq 16$ or $\lambda = 200\%$.

The main state-of-the-art codebooks for comparison with the proposed ones are the GAM codebook [21] and the Star-QAM codebook [26]⁴. This is because both [21] and [26] achieve good BER performance in downlink channels. We first analyze and present the complexity reduction of our proposed LPCBs for MPA decoder. Then, the BER performances are compared with the benchmarking codebooks in both uncoded and coded systems.

Table I compares the Δ_{\min} of the proposed codebooks, GAM and Star-QAM for the SCMA systems with overloading $\lambda = 150\%$ and $\lambda = 200\%$, respectively. In addition, since the MED is widely used as a performance metric, we also present the MED of different codebooks. Clearly, most of the proposed LPCBs enjoy larger Δ_{\min} and MED values. For example, the MEDs of proposed codebooks $A_{4,3}$ and $A_{4,2}$ of $\lambda = 150\%$ and $\lambda = 200\%$ SCMA systems, respectively, are significantly larger than that of other codebooks. It is also worth mentioning that, to our best knowledge, the proposed codebooks $A_{4,2}$ for $\lambda = 150\%$, $A_{8,4}$ and $A_{16,4}$ for $\lambda = 200\%$, enjoy the largest MED values among all existing codebooks. The details of the designed LPCBs with the largest Δ_{\min} and MED for each SCMA setting are given in Appendix C.

A. Complexity reduction with the proposed LPCBs

In this subsection, we compare the receiver complexities of the proposed LPCBs and conventional codebooks [19]–[30], referred as Non-LPCBs. The computation complexity in terms of multiplication and addition of MPA can be approximated as [46]

⁴We have also optimized the MCs that proposed in [35] with the proposed design approach. However, it is found that the resultant BER performance is far in ferier to the GAM and Star-QAM codebooks in downlink channels.

TABLE I: Comparison of the proposed codebooks in terms of Δ_{\min} , MED and I_t .

System setting (M, λ)	Codebooks	Δ_{\min}	MED	I_t (MPA)
(4, 150%)	$A_{4,2}$	1.16	1.1	1
	$A_{4,3}$	1.31	1.23	4
	Star-QAM	0.98	0.9	
	GAM	0.74	0.57	
	Huawei [45]	0.67	0.57	
(4, 200%)	$A_{4,2}$	1.05	0.96	1
	$A_{4,3}$	0.75	0.64	4
	Star-QAM	0.56	0.48	6
	GAM	0.47	0.43	
(8, 150%)	$A_{8,3}$	0.62	0.54	2
	$A_{8,4}$	0.75	0.67	4
	$A_{8,5}$	0.62	0.53	4
	$A_{8,6}$	0.51	0.46	5
	$A_{8,7}$	0.54	0.50	5
	Star-QAM	0.5	0.45	4
	GAM	0.51	0.47	6
(16, 150%)	$A_{16,4}$	0.32	0.26	1
	$A_{16,9}$	0.28	0.21	5
	Star-QAM	0.2	0.15	7
	GAM	0.2	0.16	7

$$N_m = [(d_f + 3)T^{d_f}N + (N - 2)TN]J I_t + T(N - 1)J, \quad (44)$$

$$N_a = [(d_f + 1)T^{d_f}N + (T - 1)N + (T^{d_f - 1} - 1)TN]J I_t,$$

respectively, where I_t denotes the number the number of iterations for convergence. Clearly, the decoding complexity depends on T , I_t and the system overloading. The number of iterations I_t for decoding convergence of different codebooks is given in Table I and the decoding convergence behavior is detailed in the next subsection. To proceed, we further define the normalized complexity (NC) as follows:

$$NC \triangleq \frac{\text{Number of Operations of LPCBs}}{\text{Number of Operations of Non-LPCBs}}. \quad (45)$$

As shown in Fig. 3, it is evident that the proposed LPCBs can greatly reduce the detection complexity, with more than 60% complexity reduction being achieved compared to Non-LPCBs. The gain becomes more significant as the increase of M and λ . For example, the proposed codebooks $A_{8,3}$ and $A_{16,4}$ can reduce the decoding complexity by 97.3% and

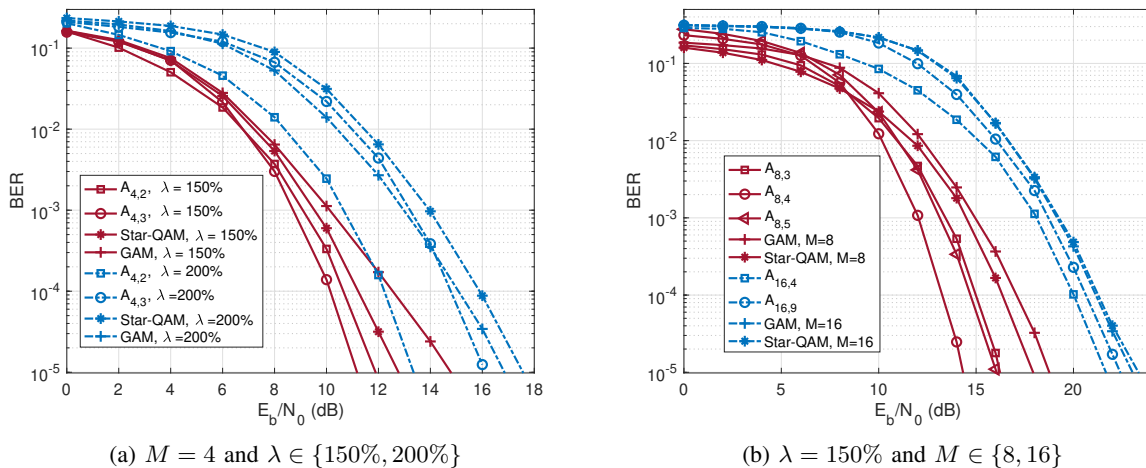


Fig. 4: BER performance of different codebooks with $\kappa \rightarrow \infty$.

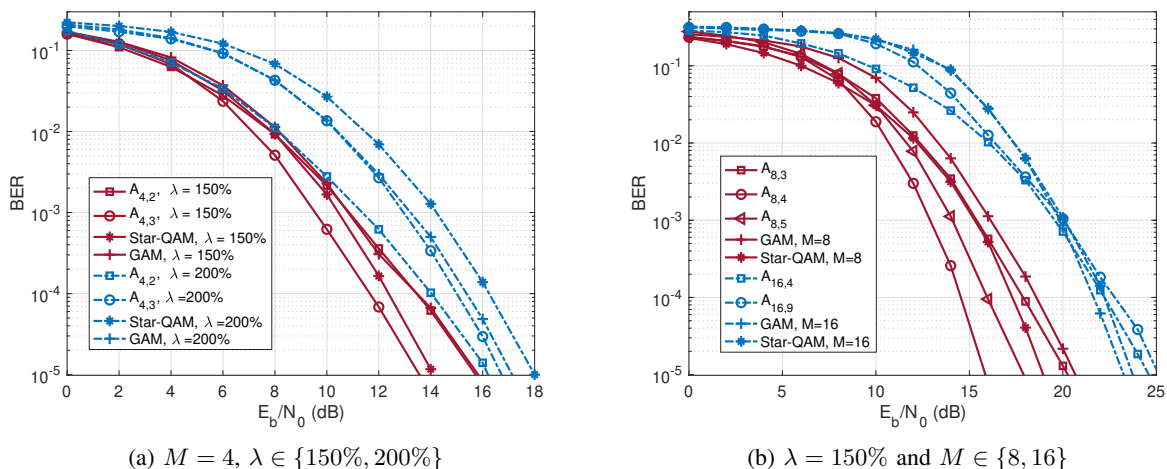


Fig. 5: BER performance of different codebooks with $\kappa = 15$.

99.7%, respectively.

B. Comparison of uncoded BER performance

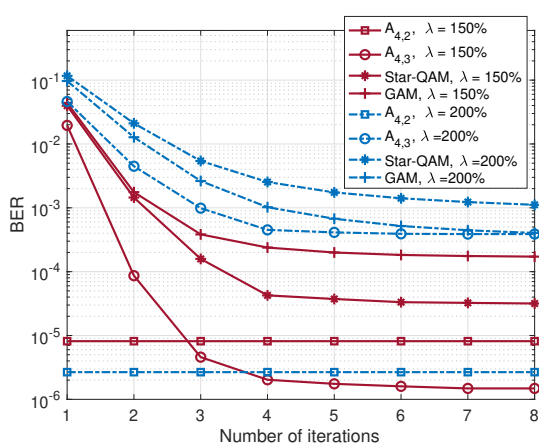
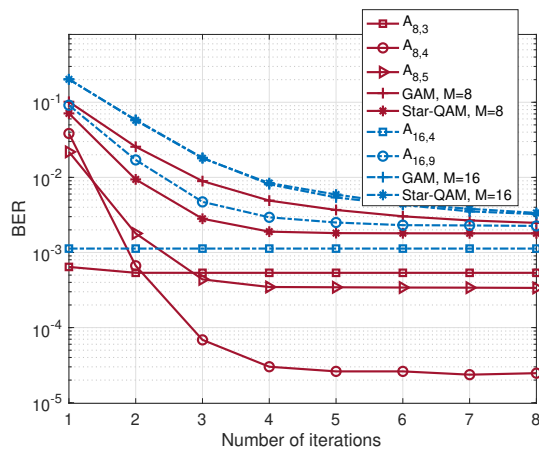
In this subsection, we evaluate the uncoded BER performance of the proposed LPCBs. As reported in [36], $\kappa \rightarrow \infty$ is assumed for open environments. In the rural and suburban scenarios with an LOS path, the Rician factor κ generally ranges from 15 to 40 [37], [38]. Thus, we consider $\kappa \rightarrow \infty$ and $\kappa = 15$ in Fig. 4 and Fig. 5, respectively.

As can be seen in Fig. 4, the proposed codebook $A_{4,3}$ for $\lambda = 150\%$ achieves about 2 dB gain over the Star-QAM codebook and 4 dB gain over the GAM codebook at $\text{BER} = 10^{-5}$, respectively. Moreover, $A_{4,3}$ for $\lambda = 200\%$ also outperforms than the Star-QAM codebook and the GAM codebook. The excellent BER advantage can be observed for the proposed $A_{4,2}$ codebook for $\lambda = 200\%$ due to large MED, which achieves about 3 dB gain over the Star-QAM codebook and 4.5 dB gain over the GAM codebook at $\text{BER}=10^{-5}$, respectively. For $M \in \{8, 16\}$ and $\lambda = 150\%$, we are interested in codebooks with less projected numbers, thus

only $A_{8,3}$, $A_{8,4}$ and $A_{8,5}$ are compared to GAM and Star-QAM codebooks in Fig. 4(b). One can see that the proposed codebooks outperform the GAM and Star-QAM codebooks significantly. Among these codebooks, $A_{8,4}$ and $A_{16,4}$ achieve the best BER performance for $M = 8$ and $M = 16$, respectively. In particular, $A_{8,4}$ has a gain about 3.8 dB over the GAM codebook and 4.2 dB over the Star-QAM codebook, respectively.

From Fig. 5, we have the following main observations: 1) For the case of $\kappa = 15$, most of the proposed LPCBs achieve good BER performance. In particular, the codebooks $A_{4,3}$ ($\lambda = 150\%$), $A_{4,2}$ ($\lambda = 200\%$), $A_{8,4}$ still outperform the GAM and Star-QAM codebooks; 2) Compared with the results in Fig. 4, the performance of LPCBs with smallest LP numbers for $\kappa = 15$, such as $A_{4,2}$ ($\lambda = 150\%$), $A_{8,3}$, $A_{16,4}$ are more likely affected by the channel fading.

Next, we examine the convergence behaviors of different codebooks with $\kappa \rightarrow \infty$ of MPA decoder in Fig. 6. It is noted that most of the proposed codebooks enjoy a faster convergence rate than the Star-QAM codebook and GAM

(a) $M = 4$, $\lambda \in \{150\%, 200\%\}$ and $E_b/N_0 = 12$ dB(b) $\lambda = 150\%$, $M = 8$ ($E_b/N_0 = 14$ dB) and $M = 16$ ($E_b/N_0 = 18$ dB)Fig. 6: Number of iterations vs. BER performance of different codebooks ($\kappa \rightarrow \infty$).

codebook⁵. With reduced projected numbers (T), less message propagation between function nodes and variable nodes are required during MPA iteration, thus leading to less iterations for convergence. In particular, the proposed codebooks $A_{4,2}$, $A_{8,3}$ and $A_{16,4}$ for $\lambda = 150\%$, and $A_{4,2}$ for $\lambda = 200\%$ only need about one iteration to converge. The decoding can be carried out in a single shot for these codebooks and the decoding complexity is significantly reduced compared to other codebooks.

C. Comparison of coded BER performance

In this subsection, we compare the coded BER performances of the proposed codebooks with the GAM and Star-QAM codebooks. In some scenarios, such as dense urban and urban areas with an LOS path, κ is relatively small [36]–[38]. Hence, we set κ with a wide range. Considering the short-packet nature of IoT networks, we apply the 5G NR LDPC codes with small block length [7], [47], as specified in TS38.212 [48]. The detailed simulation settings are given in Table II and the simulated BER performance are depicted in Fig. 7.

In Fig. 7(a), the proposed codebook $A_{4,2}$ and $A_{4,3}$ show better performance than the GAM and Star-QAM codebooks for $\kappa = 30$. In particular, the $A_{4,3}$ outperforms Star-QAM codebook by 1 dB gain at $\text{BER} = 10^{-4}$. When there exists severe fading, i.e., $\kappa = 2$, the error performance of $A_{4,2}$ deteriorates, however, the proposed $A_{4,3}$ still achieves similar BER performance with the Star-QAM codebook and performs slightly better in the low E_b/N_0 range. By observing the slopes of the curves, the GAM codebook enjoys a larger diversity gain than the low projected codebooks. This is because some constellation points in the LPCBs are overlapped in order to reduce the decoding complexity, thus the diversity between these constellation pairs may be reduced. However, we show that by properly designing the MC and maximising the coding gain, most of the proposed LPCBs can still achieve good BER performance for $\kappa = 2$.

⁵For other values of κ , we also observe the similar result that the proposed LPCBs require less iterations for convergence.

TABLE II: Simulation Parameters

Parameters	Values
Transmission	Downlink
Channel model	Rician fading channel, $\kappa = 2, 30$
SCMA setting	$\lambda = 150\%$ and $\lambda = 200\%$
Channel coding	5G NR LDPC codes with rate of 0.8462 and block length of 260
Codebooks	The same codebooks presented in Fig. 4 and Fig. 5
Receiver	Turbo-MPA: 1 MPA iteration for $A_{4,2}$ ($\lambda = 150\%$), $A_{4,2}$ ($\lambda = 200\%$), $A_{8,3}$ and $A_{16,4}$, and 4 MPA iterations for other codebooks, 5 BICM iterations

For the 8-ary and 16-ary codebooks shown in Fig. 7(b) and Fig. 7(c), respectively, BER trends similar to that of the 4-ary codebook are observed. The proposed codebooks outperform the GAM and Star-QAM codebooks for $\kappa = 30$, whereas the error performance of the proposed codebooks with least projection numbers deteriorate for the case of $\kappa = 2$. It is interesting to see the proposed codebook $A_{8,4}$ and $A_{16,4}$ achieve the best coded BER performance for both $\kappa = 30$ and $\kappa = 2$ among all the codebooks owing to the well optimized bit labeling and large coding gain. For example, $A_{8,4}$ achieves about 3.6 dB gain over the GAM codebook and 1.5 dB gain over the Star-QAM codebook for $\kappa = 30$, and achieves about 2 dB gain over the GAM codebook and 1 dB gain over the Star-QAM codebook for $\kappa = 2$ at $\text{BER} = 10^{-4}$, respectively.

As shown in Fig. 7(d), for the SCMA system with $\lambda = 200\%$, the proposed codebook $A_{4,2}$ achieves about 1 dB gain compared to the GAM with $\kappa = 30$ due to the very large coding gain, however, the BER curve degrades earlier than others for $\kappa = 2$. The superiority of the proposed codebooks mainly lies in the huge reduction of complexity, especially in largely overloaded system.

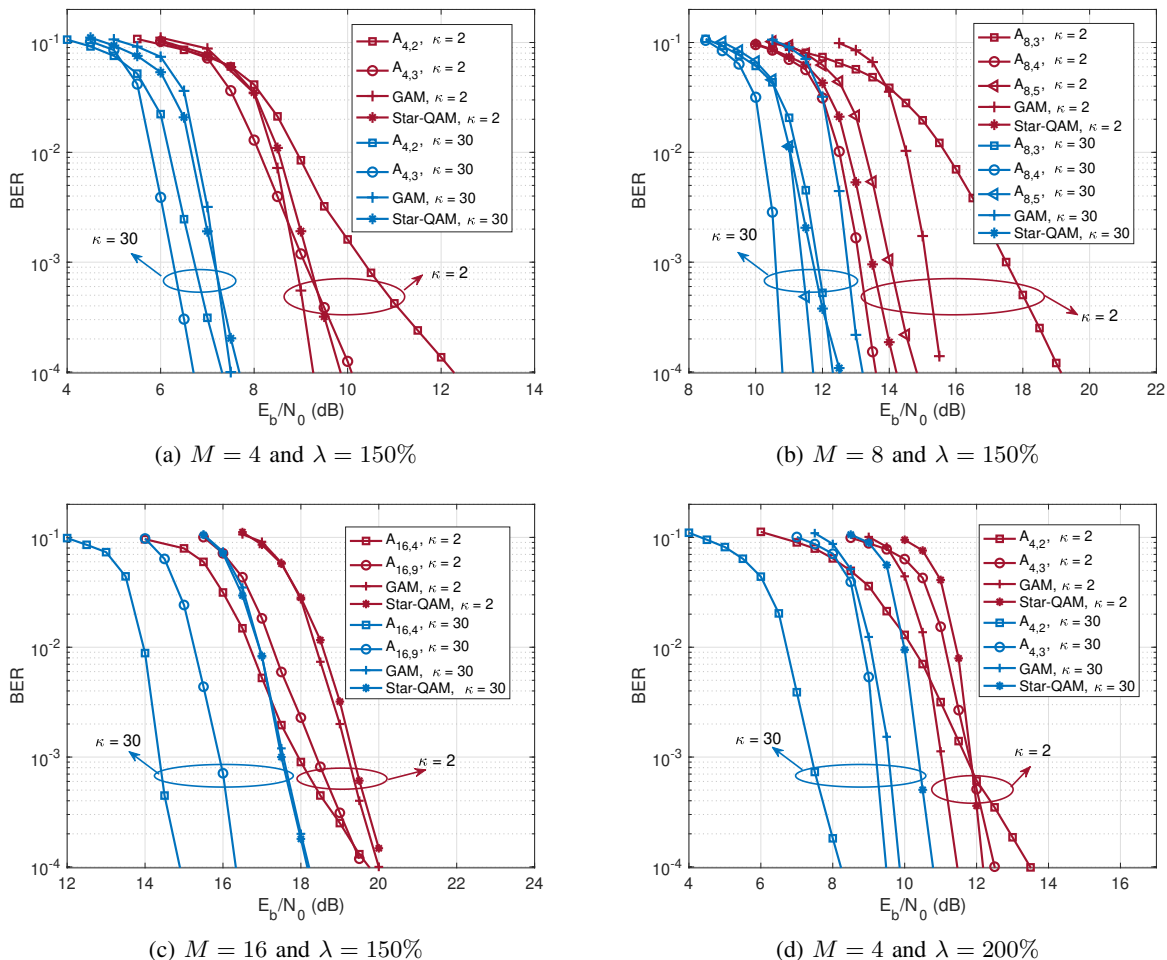


Fig. 7: LDPC coded BER performance comparison of different codebooks.

VI. CONCLUSION

In this paper, we introduced a novel class of SCMA codebooks that can significantly reduce the decoding complexity while achieving good BER performance for downlink S-LoT networks. We analysed the corresponding pairwise error probability of SCMA transmissions under a generalized Rician fading channel model and derived the codebook design criteria. To reduce the decoding complexity, we have proposed to construct the MC with LPGAM by allowing several overlapped constellation points in each dimension. In addition, we developed an efficient codebook design approach, including permutation, bit labeling, sparse codebook construction and parameter optimization. Numerical results demonstrated the benefits of proposed codebook in terms of complexity reduction and BER performance improvements in different S-LoT environments. In particular, some codebooks (e.g., $A_{4,2}$, $A_{4,3}$, $A_{8,4}$ and $A_{16,4}$ for $\lambda = 150\%$ system and $A_{4,2}$ for $\lambda = 200\%$ system) achieve significant performance improvements for typical κ values in open, rural and suburban environments, and significant complexity reduction compared to the existing codebooks.

APPENDIX A PROOF OF THE LEMMA 1

For an M -ary \mathcal{C}_{MC} , the primary design rule is that the resultant MC should be uniquely separable. Namely, giving arbitrary two vectors $\bar{\mathbf{c}}_i$ and $\bar{\mathbf{c}}_l$ in \mathcal{C}_{MC} , we have $\bar{\mathbf{c}}_i \neq \bar{\mathbf{c}}_l$ with $i \neq l$. Hence, for the basic constellation with T distinct points, the N -dimensional constellation with maximum size can be constructed is T^N , where construction is given by the Cartesian product over the basic constellation. For example, consider $T = 2$ and $N = 2$ and assume that the designed basic constellation $\mathcal{A}_2 = \{-a, +a\} \in \mathbb{C}$, obviously, the unique decodable 2-dimensional constellation with maximum size can be generated as $\mathcal{A}_2 \times \mathcal{A}_2 \rightarrow \mathcal{C}_{MC}$, i.e.,

$$\mathcal{C}_{MC} = \begin{bmatrix} -a & +a & -a & +a \\ -a & -a & +a & +a \end{bmatrix}. \quad (46)$$

Therefore, for the given M and N , the LP number should satisfy $\lceil \sqrt[N]{M} \rceil \leq T \leq M$, and for the case of $T = \sqrt[N]{M} \in \mathbb{Z}$, the construction of \mathcal{C}_{MC} is given by the Cartesian product of \mathcal{A}_T .

This completes the proof of Lemma 1.

APPENDIX B
PROOF OF THE LEMMA 3

The proof of Lemma 3 can be proceed in two steps as follows.

In the first step, we show that Φ_{M^J} can be expressed as the Cartesian product of \mathcal{S}_{sum} . To proceed, we rewrite the constellation superposition set as

$$\Phi_{M^J} = \{\mathbf{w} = \mathbf{x}_1 + \mathbf{x}_2 + \cdots + \mathbf{x}_J | \forall \mathbf{x}_j \in \mathcal{X}_j, j = 1, 2, \dots, J\}, \quad (47)$$

where the mapping rule is given by $g_\Phi: \mathcal{X}_1 + \cdots + \mathcal{X}_J \rightarrow \Phi_{M^J}$. Similarly, we have $g_S: z_1 \mathcal{A}_T + \cdots + z_{d_f} \mathcal{A}_T \rightarrow \mathcal{S}_{\text{sum}}$. In fact, the constellation superposition process is characterized by a Cartesian product mapping. The Lemma 1 reveals that for $T = \sqrt[N]{M}$, the mapping $f_{\text{MC}}: \mathcal{A}_T \times \cdots \times \mathcal{A}_T \rightarrow \mathcal{C}_{\text{MC}}$ is a Cartesian product. Accordingly, the mapping $f_{\mathcal{C}_j}: z_1^{(j)} \mathcal{A}_T \times \cdots \times z_N^{(j)} \mathcal{A}_T \rightarrow \mathcal{C}_j$ is also a Cartesian product, where $z_n^{(j)}$ is the j th user's constellation operator. Based on $f_{\mathcal{C}_j}$, we can rewrite g_Φ as

$$g_\Phi: \mathbf{V}_1 f_{\mathcal{C}_1} + \cdots + \mathbf{V}_J f_{\mathcal{C}_J} \rightarrow \Phi_{M^J}. \quad (48)$$

(48) indicates that Φ_{M^J} is obtained by the two steps: 1) Mapping the 1-dimension LPGAM \mathcal{A}_T to \mathcal{C}_j ; 2) Constellation superposition. Since the two steps are both characterized by the Cartesian product, the changes in the order of the two steps will not affect the result of Φ_{M^J} . Namely, Φ_{M^J} can also be obtained by: 1) Constellation superposition based on LPGAM, i.e., $g_S: z_1 \mathcal{A}_T + \cdots + z_{d_f} \mathcal{A}_T \rightarrow \mathcal{S}_{\text{sum}}$; 2) Obtain Φ_{M^J} by performing Cartesian product over \mathcal{S}_{sum} , i.e.,

$$f_\Phi: \mathcal{S}_{\text{sum}}^{(1)} \times \cdots \times \mathcal{S}_{\text{sum}}^{(K)} \rightarrow \Phi_{M^J}. \quad (49)$$

In Step 2, we show that maximize $\text{MED}(\mathcal{S}_{\text{sum}})$ is equivalent to maximizing $\Delta_{\min}(\mathcal{X}_{\lambda, M, T})$. Let \mathbf{w} and $\hat{\mathbf{w}}$ be two superimposed codeword vectors, and define

$$G \triangleq \min_{\mathbf{w}, \hat{\mathbf{w}}, \mathbf{w} \neq \hat{\mathbf{w}}} \underbrace{\sum_{k=1}^K \text{Ind}(\tau_{\mathbf{w} \rightarrow \hat{\mathbf{w}}}(k))}_{G(\mathbf{w} \rightarrow \hat{\mathbf{w}})}, \quad (50)$$

where $\tau_{\mathbf{w} \rightarrow \hat{\mathbf{w}}}(k) = |w(k) - \hat{w}(k)|^2$, and $w(k)$ is the k th entry of \mathbf{w} . Obviously, since Φ_{M^J} can be generated by the Cartesian product of \mathcal{S}_{sum} , we have $G = 1$ and the MED of Φ_{M^J} equals to $\text{MED}(\mathcal{S}_{\text{sum}})$. Assume \mathbf{w}_m and \mathbf{w}_n are the two vectors that achieve the MED value, and $\tau_{\mathbf{w}_m \rightarrow \mathbf{w}_n}(k') \neq 0$. Accordingly, we obtain $\tau_{\mathbf{w}_m \rightarrow \mathbf{w}_n}(k') = \text{MED}(\mathcal{S}_{\text{sum}})$. This also indicates that for arbitrary two vectors \mathbf{w} and $\hat{\mathbf{w}}$, $\tau_{\mathbf{w} \rightarrow \hat{\mathbf{w}}}(k) = 0$ or $\tau_{\mathbf{w} \rightarrow \hat{\mathbf{w}}}(k) \geq \text{MED}(\mathcal{S}_{\text{sum}})$, $k = 1, 2, \dots, K$.

Based on (15), $d_{\mathbf{w} \rightarrow \hat{\mathbf{w}}}^2$ is an increasing function of $G(\mathbf{w} \rightarrow \hat{\mathbf{w}})$ and $\tau_{\mathbf{w}_m \rightarrow \mathbf{w}_n}(k)$. Hence, (38) achieves the minimum value at \mathbf{w}_m and \mathbf{w}_n , where $G = 1$ and $\tau_{\mathbf{w}_m \rightarrow \mathbf{w}_n}(k') = \text{MED}(\mathcal{S}_{\text{sum}})$. Therefore, improving $\text{MED}(\mathcal{S}_{\text{sum}})$ is equivalent to increasing $\Delta_{\min}(\mathcal{X}_{\lambda, M, T})$.

This completes the proof of Lemma 3.

APPENDIX C
THE PROPOSED LPCBS

The proposed LPCBs of $A_{4,3}$ ($\lambda = 150\%$), $A_{4,2}$ ($\lambda = 200\%$) and $A_{8,4}$ ($\lambda = 150\%$) are presented. For $M = 4$,

the four columns of in \mathcal{X}_j denote the codewords with labelled by 00, 01, 10, 11. Similarly, for $M = 8$, the eight columns represent the codewords labelled by 000, 001, 010, 011, 100, 101, 110, 111.

A. The proposed LPCB $A_{4,3}$ ($\lambda = 150\%$)

$$\begin{aligned} \mathcal{X}_1 &= \begin{bmatrix} 0 & 0.0850 + 1.0324i & 0 & 0 \\ 0 & 0 & 0 & 1.0841 + 0.0000i \\ 0 & 0 & 0 & -1.0841 + 0.0000i \\ 0 & -0.0850 - 1.0324i & 0 & 0 \end{bmatrix}^T, \\ \mathcal{X}_2 &= \begin{bmatrix} 0.0850 + 1.0324i & 0 & 0 & 0 \\ 0 & 0 & 1.0841 + 0.0000i & 0 \\ 0 & 0 & -1.0841 + 0.0000i & 0 \\ -0.0850 - 1.0324i & 0 & 0 & 0 \end{bmatrix}^T, \\ \mathcal{X}_3 &= \begin{bmatrix} -0.7156 + 0.4894i & 0 & 0 & 0 \\ 0 & -0.7156 + 0.4894i & 0 & 0 \\ 0 & 0.7156 - 0.4894i & 0 & 0 \\ 0.7156 - 0.4894i & 0 & 0 & 0 \end{bmatrix}^T, \\ \mathcal{X}_4 &= \begin{bmatrix} 0 & 0 & -0.7156 + 0.4894i & 0 \\ 0 & 0 & 0 & -0.7156 + 0.4894i \\ 0 & 0 & 0 & 0.7156 - 0.4894i \\ 0 & 0 & 0.7156 - 0.4894i & 0 \end{bmatrix}^T, \\ \mathcal{X}_5 &= \begin{bmatrix} 1.0841 + 0.0000i & 0 & 0 & 0 \\ 0 & 0 & 0 & 0.0850 + 1.0324i \\ 0 & 0 & 0 & -0.0850 - 1.0324i \\ -1.0841 + 0.0000i & 0 & 0 & 0 \end{bmatrix}^T, \\ \mathcal{X}_6 &= \begin{bmatrix} 0 & 1.0841 + 0.0000i & 0 & 0 \\ 0 & 0 & 0.0850 + 1.0324i & 0 \\ 0 & 0 & -0.0850 - 1.0324i & 0 \\ 0 & -1.0841 + 0.0000i & 0 & 0 \end{bmatrix}^T. \end{aligned}$$

B. The proposed LPCB $A_{4,2}$ ($\lambda = 200\%$)

$$\begin{aligned} \mathcal{X}_1 &= \begin{bmatrix} 0.6576 + 0.6755i & 0.5852 - 0.5696i & 0 & 0 & 0 \\ 0.6576 + 0.6755i & -0.5852 + 0.5696i & 0 & 0 & 0 \\ -0.6576 - 0.6755i & 0.5852 - 0.5696i & 0 & 0 & 0 \\ -0.6576 - 0.6755i & -0.5852 + 0.5696i & 0 & 0 & 0 \end{bmatrix}^T, \\ \mathcal{X}_2 &= \begin{bmatrix} -0.1282 + 0.4536i & 0 & -0.3288 - 0.3378i & 0 & 0 \\ -0.1282 + 0.4536i & 0 & 0.3288 + 0.3378i & 0 & 0 \\ 0.1282 - 0.4536i & 0 & -0.3288 - 0.3378i & 0 & 0 \\ 0.1282 - 0.4536i & 0 & 0.3288 + 0.3378i & 0 & 0 \end{bmatrix}^T, \\ \mathcal{X}_3 &= \begin{bmatrix} 0.3288 + 0.3378i & 0 & 0 & 0.1282 - 0.4536i & 0 \\ 0.3288 + 0.3378i & 0 & 0 & -0.1282 + 0.4536i & 0 \\ -0.3288 - 0.3378i & 0 & 0 & 0.1282 - 0.4536i & 0 \\ -0.3288 - 0.3378i & 0 & 0 & -0.1282 + 0.4536i & 0 \end{bmatrix}^T, \\ \mathcal{X}_4 &= \begin{bmatrix} -0.5852 + 0.5696i & 0 & 0 & 0 & -0.6576 - 0.6755i \\ -0.5852 + 0.5696i & 0 & 0 & 0 & 0.6576 + 0.6755i \\ 0.5852 - 0.5696i & 0 & 0 & 0 & -0.6576 - 0.6755i \\ 0.5852 - 0.5696i & 0 & 0 & 0 & 0.6576 + 0.6755i \end{bmatrix}^T, \\ \mathcal{X}_5 &= \begin{bmatrix} 0 & 0.6576 + 0.6755i & 0.5852 - 0.5696i & 0 & 0 \\ 0 & 0.6576 + 0.6755i & -0.5852 + 0.5696i & 0 & 0 \\ 0 & -0.6576 - 0.6755i & 0.5852 - 0.5696i & 0 & 0 \\ 0 & -0.6576 - 0.6755i & -0.5852 + 0.5696i & 0 & 0 \end{bmatrix}^T, \\ \mathcal{X}_6 &= \begin{bmatrix} 0 & -0.1282 + 0.4536i & 0 & -0.3288 - 0.3378i & 0 \\ 0 & -0.1282 + 0.4536i & 0 & 0.3288 + 0.3378i & 0 \\ 0 & 0.1282 - 0.4536i & 0 & -0.3288 - 0.3378i & 0 \\ 0 & 0.1282 - 0.4536i & 0 & 0.3288 + 0.3378i & 0 \end{bmatrix}^T, \\ \mathcal{X}_7 &= \begin{bmatrix} 0 & 0.3288 + 0.3378i & 0 & 0 & 0.1282 - 0.4536i \\ 0 & 0.3288 + 0.3378i & 0 & 0 & -0.1282 + 0.4536i \\ 0 & -0.3288 - 0.3378i & 0 & 0 & 0.1282 - 0.4536i \\ 0 & -0.3288 - 0.3378i & 0 & 0 & -0.1282 + 0.4536i \end{bmatrix}^T, \end{aligned}$$

$$\mathcal{X}_8 = \begin{bmatrix} 0 & 0 & 0.6576 + 0.6755i & 0.5852 - 0.5696i & 0 \\ 0 & 0 & 0.6576 + 0.6755i & -0.5852 + 0.5696i & 0 \\ 0 & 0 & -0.6576 - 0.6755i & 0.5852 - 0.5696i & 0 \\ 0 & 0 & -0.6576 - 0.6755i & -0.5852 + 0.5696i & 0 \end{bmatrix}^T,$$

$$\mathcal{X}_9 = \begin{bmatrix} 0 & 0 & -0.1282 + 0.4536i & 0 & -0.3288 - 0.3378i \\ 0 & 0 & -0.1282 + 0.4536i & 0 & 0.3288 + 0.3378i \\ 0 & 0 & 0.1282 - 0.4536i & 0 & -0.3288 - 0.3378i \\ 0 & 0 & 0.1282 - 0.4536i & 0 & 0.3288 + 0.3378i \end{bmatrix}^T,$$

$$\mathcal{X}_{10} = \begin{bmatrix} 0 & 0 & 0 & 0.6576 + 0.6755i & 0.5852 - 0.5696i \\ 0 & 0 & 0 & 0.6576 + 0.6755i & -0.5852 + 0.5696i \\ 0 & 0 & 0 & -0.6576 - 0.6755i & 0.5852 - 0.5696i \\ 0 & 0 & 0 & -0.6576 - 0.6755i & -0.5852 + 0.5696i \end{bmatrix}^T.$$

C. The proposed LPCB $A_{8,4}$ ($\lambda = 150\%$)

$$\mathcal{X}_1 = \begin{bmatrix} 0 & 0.3202 + 0.3995i & 0 & 0.0863 - 0.7668i \\ 0 & 0.3202 + 0.3995i & 0 & -0.6940 + 0.4385i \\ 0 & -0.1187 + 0.5316i & 0 & 0.6940 - 0.4385i \\ 0 & -0.1187 + 0.5316i & 0 & -0.0863 + 0.7668i \\ 0 & 0.1187 - 0.5316i & 0 & 0.0863 - 0.7668i \\ 0 & 0.1187 - 0.5316i & 0 & -0.6940 + 0.4385i \\ 0 & -0.3202 - 0.3995i & 0 & 0.6940 - 0.4385i \\ 0 & -0.3202 - 0.3995i & 0 & -0.0863 + 0.7668i \end{bmatrix}^T,$$

$$\mathcal{X}_2 = \begin{bmatrix} 0.3202 + 0.3995i & 0 & 0.0863 - 0.7668i & 0 \\ 0.3202 + 0.3995i & 0 & -0.6940 + 0.4385i & 0 \\ -0.1187 + 0.5316i & 0 & 0.6940 - 0.4385i & 0 \\ -0.1187 + 0.5316i & 0 & -0.0863 + 0.7668i & 0 \\ 0.1187 - 0.5316i & 0 & 0.0863 - 0.7668i & 0 \\ 0.1187 - 0.5316i & 0 & -0.6940 + 0.4385i & 0 \\ -0.3202 - 0.3995i & 0 & 0.6940 - 0.4385i & 0 \\ -0.3202 - 0.3995i & 0 & -0.0863 + 0.7668i & 0 \end{bmatrix}^T,$$

$$\mathcal{X}_3 = \begin{bmatrix} -0.7410 - 0.0249i & 0.7410 + 0.0249i & 0 & 0 \\ -0.7410 - 0.0249i & -0.4723 - 0.6317i & 0 & 0 \\ -0.4723 - 0.6317i & 0.4723 + 0.6317i & 0 & 0 \\ -0.4723 - 0.6317i & -0.7410 - 0.0249i & 0 & 0 \\ 0.4723 + 0.6317i & 0.7410 + 0.0249i & 0 & 0 \\ 0.4723 + 0.6317i & -0.4723 - 0.6317i & 0 & 0 \\ 0.7410 + 0.0249i & 0.4723 + 0.6317i & 0 & 0 \\ 0.7410 + 0.0249i & -0.7410 - 0.0249i & 0 & 0 \end{bmatrix}^T,$$

$$\mathcal{X}_4 = \begin{bmatrix} 0 & 0 & -0.7410 - 0.0249i & 0.7410 + 0.0249i \\ 0 & 0 & -0.7410 - 0.0249i & -0.4723 - 0.6317i \\ 0 & 0 & -0.4723 - 0.6317i & 0.4723 + 0.6317i \\ 0 & 0 & -0.4723 - 0.6317i & -0.7410 - 0.0249i \\ 0 & 0 & 0.4723 + 0.6317i & 0.7410 + 0.0249i \\ 0 & 0 & 0.4723 + 0.6317i & -0.4723 - 0.6317i \\ 0 & 0 & 0.7410 + 0.0249i & 0.4723 + 0.6317i \\ 0 & 0 & 0.7410 + 0.0249i & -0.7410 - 0.0249i \end{bmatrix}^T,$$

$$\mathcal{X}_5 = \begin{bmatrix} -0.0863 + 0.7668i & 0 & 0 & -0.3202 - 0.3995i \\ -0.0863 + 0.7668i & 0 & 0 & -0.1187 + 0.5316i \\ -0.6940 + 0.4385i & 0 & 0 & 0.1187 - 0.5316i \\ -0.6940 + 0.4385i & 0 & 0 & 0.3202 + 0.3995i \\ 0.6940 - 0.4385i & 0 & 0 & -0.3202 - 0.3995i \\ 0.6940 - 0.4385i & 0 & 0 & -0.1187 + 0.5316i \\ 0.0863 - 0.7668i & 0 & 0 & 0.1187 - 0.5316i \\ 0.0863 - 0.7668i & 0 & 0 & 0.3202 + 0.3995i \end{bmatrix}^T,$$

$$\mathcal{X}_6 = \begin{bmatrix} 0 & -0.0863 + 0.7668i & -0.3202 - 0.3995i & 0 \\ 0 & -0.0863 + 0.7668i & -0.1187 + 0.5316i & 0 \\ 0 & -0.6940 + 0.4385i & 0.1187 - 0.5316i & 0 \\ 0 & -0.6940 + 0.4385i & 0.3202 + 0.3995i & 0 \\ 0 & 0.6940 - 0.4385i & -0.3202 - 0.3995i & 0 \\ 0 & 0.6940 - 0.4385i & -0.1187 + 0.5316i & 0 \\ 0 & 0.0863 - 0.7668i & 0.1187 - 0.5316i & 0 \\ 0 & 0.0863 - 0.7668i & 0.3202 + 0.3995i & 0 \end{bmatrix}^T.$$

REFERENCES

- [1] M. De Sanctis, E. Cianca, G. Araniti, I. Bisio, and R. Prasad, "Satellite communications supporting Internet of remote things," *IEEE Internet Things J.*, vol. 3, no. 1, pp. 113–123, Oct. 2016.
- [2] A. Ghasempour, "Internet of things in smart grid: Architecture, applications, services, key technologies, and challenges," *Inventions*, vol. 4, no. 1, p. 22, Feb. 2019.
- [3] C. Wang, L. Liu, H. Ma, and D. Xia, "A joint optimization scheme for hybrid MAC layer in LEO satellite supported IoT," *IEEE Internet Things J.*, vol. 8, no. 15, pp. 11 822–11 833, Mar. 2021.
- [4] X. Zhu, C. Jiang, L. Kuang, N. Ge, and J. Lu, "Non-orthogonal multiple access based integrated terrestrial-satellite networks," *IEEE J. Sel. Areas Commun.*, vol. 35, no. 10, pp. 2253–2267, Jul. 2017.
- [5] L. Yu, Z. Liu, M. Wen, D. Cai, S. Dang, Y. Wang, and P. Xiao, "Sparse code multiple access for 6G wireless communication networks: Recent advances and future directions," *IEEE Commun. Stand. Mag.*, vol. 5, no. 2, pp. 92–99, Jun. 2021.
- [6] S. R. Islam, N. Avazov, O. A. Dobre, and K.-S. Kwak, "Power-domain non-orthogonal multiple access (NOMA) in 5G systems: Potentials and challenges," *IEEE Commun. Surveys Tuts*, vol. 19, no. 2, pp. 721–742, Oct. 2016.
- [7] Z. Liu and L.-L. Yang, "Sparse or dense: A comparative study of code-domain NOMA systems," *IEEE Trans. Wireless Commun.*, vol. 20, no. 8, pp. 4768–4780, Aug. 2021.
- [8] M. Taherzadeh, H. Nikopour, A. Bayesteh, and H. Baligh, "SCMA codebook design," in *Proc. IEEE 80th Veh. Techno. Conf. (VTC2014-Fall)*, Vancouver, Canada, Dec. 2014, pp. 1–5.
- [9] R. Hoshyar, F. P. Wathan, and R. Tafazolli, "Novel low-density signature for synchronous CDMA systems over awgn channel," *IEEE J. Sel. Areas Commun.*, vol. 56, no. 4, pp. 1616–1626, Mar. 2008.
- [10] Q. Luo *et al.*, "An error rate comparison of power domain non-orthogonal multiple access and sparse code multiple access," *IEEE Open J. Commun. Soc.*, vol. 2, no. 4, pp. 500–511, Mar. 2021.
- [11] S. Moon, H.-S. Lee, and J.-W. Lee, "SARA: Sparse code multiple access-applied random access for IoT devices," *IEEE Internet Things J.*, vol. 5, no. 4, pp. 3160–3174, May 2018.
- [12] L. Miuccio, D. Panno, and S. Riolo, "Joint control of random access and dynamic uplink resource dimensioning for massive MTC in 5G NR based on SCMA," *IEEE Internet Things J.*, vol. 7, no. 6, pp. 5042–5063, Feb. 2020.
- [13] P. Li, G. Cui, and W. Wang, "Asynchronous flipped grant-free SCMA for satellite-based Internet of things communication networks," *Applied Sciences*, vol. 9, no. 2, p. 335, Jan. 2019.
- [14] K. Lai, J. Lei, Y. Deng, L. Wen, G. Chen, and W. Liu, "Analyzing uplink grant-free sparse code multiple access system in massive IoT networks," *IEEE Internet Things J.*, pp. 1–1, Sep. 2021.
- [15] Y. Gui, L. Zhu, and J. Liu, "SCMA secure communication scheme for satellite system based on distance spectrum," in *2021 IEEE Wireless Commun. Net. Conf. Workshops (WCNCW)*. Nanjing, China: IEEE, 2021, pp. 1–6.
- [16] H. Nikopour and H. Baligh, "Sparse code multiple access," in *Proc. IEEE 24th Int. Symp. Pers., Indoor, Mobile Radio Commun. (PIMRC)*, London, U.K., Sep. 2013, pp. 332–336.
- [17] L. Chai, Z. Liu, P. Xiao, A. Maaref, and L. Bai, "An improved EPA based receiver design for uplink LDPC coded SCMA system," *IEEE Wireless Commun. Lett.*, Mar. 2022.
- [18] M. Vameghestahbanati, I. D. Marsland, R. H. Gohary, and H. Yanikomeroglu, "Multidimensional constellations for uplink SCMA systems—a comparative study," *IEEE Commun. Surveys Tuts*, vol. 21, no. 3, pp. 2169–2194, Apr. 2019.
- [19] L. Yu, X. Lei, P. Fan, and D. Chen, "An optimized design of SCMA codebook based on star-qam signaling constellations," in *Proc. 2 Int. Conf. Wireless Commun. Signal Processing (WCSP)*, Nanjing, China, Oct. 2015, pp. 1–5.
- [20] D. Cai, P. Fan, X. Lei, Y. Liu, and D. Chen, "Multi-dimensional SCMA codebook design based on constellation rotation and interleaving," in *Proc. IEEE 83rd Veh. Techno. Conf. (VTC Spring)*, Nanjing, China, Jul. 2016, pp. 1–5.
- [21] Z. Mheich, L. Wen, P. Xiao, and A. Maaref, "Design of SCMA codebooks based on golden angle modulation," *IEEE Trans. Veh. Technol.*, vol. 68, no. 2, pp. 1501–1509, Dec. 2018.
- [22] H. Yan, H. Zhao, Z. Lv, and H. Yang, "A top-down SCMA codebook design scheme based on lattice theory," in *Proc. IEEE 27th Int. Symp. Pers., Indoor, Mobile Radio Commun. (PIMRC)*, Valencia, Spain, Dec. 2016, pp. 1–5.
- [23] M. Alam and Q. Zhang, "Designing optimum mother constellation and codebooks for SCMA," in *Proc. 2017 IEEE Int. Conf. Commun. (ICC)*, Paris, France, Jul. 2017, pp. 1–6.
- [24] K. Deka, M. Priyadarsini, S. Sharma, and B. Beferull-Lozano, "Design of SCMA codebooks using differential evolution," in *Proc. 2020 IEEE*

- Int. Conf. Commun. Workshops (ICC Workshops)*, Dublin, Ireland, Jul. 2020, pp. 1–7.
- [25] S. Sharma, K. Deka, V. Bhatia, and A. Gupta, “SCMA codebook based on optimization of mutual information and shaping gain,” in *Proc. IEEE Global Commun. Conf. (GLOBELCOM)*, Abu Dhabi, United Arab Emirates, Aug. 2018, pp. 1–6.
- [26] L. Yu, P. Fan, D. Cai, and Z. Ma, “Design and analysis of SCMA codebook based on Star-QAM signaling constellations,” *IEEE Trans. Veh. Technol.*, vol. 67, no. 11, pp. 10 543–10 553, Aug. 2018.
- [27] V. P. Klimentyev and A. B. Sergienko, “SCMA codebooks optimization based on genetic algorithm,” in *Proc. 23th European Wireless Conf.*, Dresden, Germany, Aug. 2017, pp. 1–6.
- [28] X. Zhang, D. Zhang, L. Yang, G. Han, H.-H. Chen, and D. Zhang, “SCMA codebook design based on uniquely decomposable constellation groups,” *IEEE Trans. Wireless Commun.*, vol. 20, no. 8, pp. 4828–4842, Mar. 2021.
- [29] X. Li, Z. Gao, Y. Gui, Z. Liu, P. Xiao, and L. Yu, “Design of power-imbalanced scma codebook,” *IEEE Tran. Veh. Technol.*, vol. 71, no. 2, pp. 2140–2145, Feb. 2022.
- [30] Y.-M. Chen and J.-W. Chen, “On the design of near-optimal sparse code multiple access codebooks,” *IEEE Trans. Commun.*, vol. 68, no. 5, pp. 2950–2962, Feb. 2020.
- [31] J. Boutros, E. Viterbo, C. Rastello, and J.-C. Belfiore, “Good lattice constellations for both Rayleigh fading and Gaussian channels,” *IEEE Trans. Inf. Theory*, vol. 42, no. 2, pp. 502–518, Mar. 1996.
- [32] M. Vameghestahbanati, I. D. Marsland, R. H. Gohary, and H. Yanikomeroglu, “Multidimensional constellations for uplink SCMA systems—A comparative study,” *IEEE Commun. Surveys Tuts*, vol. 21, no. 3, pp. 2169–2194, Apr. 2019.
- [33] C. Huang, B.-C. Su, T. Lin, and Y. Huang, “Downlink SCMA codebook design with low error rate by maximizing minimum Euclidean distance of superimposed codewords,” *IEEE Trans. Veh. Technol.*, 2022.
- [34] A. Bayesteh, H. Nikopour, M. Taherzadeh, H. Baligh, and J. Ma, “Low complexity techniques for SCMA detection,” in *Proc. IEEE Global commun. conf. (GLOBELCOM)*, San Diego, CA, USA, Feb. 2015, pp. 1–6.
- [35] J. Bao, Z. Ma, M. Xiao, T. A. Tsiftsis, and Z. Zhu, “Bit-interleaved coded SCMA with iterative multiuser detection: Multidimensional constellations design,” *IEEE Trans. Commun.*, vol. 66, no. 11, pp. 5292–5304, Dec. 2017.
- [36] 3GPP TS 38.811, Rel. 15 , “5G NR, study on new radio (NR) to support non-terrestrial networks,” Jul. 2018. [Online]. Available: <https://www.3gpp.org/ftp/Specs/archive/38series/38.811>
- [37] E. Lutz, D. Cygan, M. Dippold, F. Dolainsky, and W. Papke, “The land mobile satellite communication channel-recording, statistics, and channel model,” *IEEE Trans. Veh. Technol.*, vol. 40, no. 2, pp. 375–386, May 1991.
- [38] B. Vucetic and J. Du, “Channel modeling and simulation in satellite mobile communication systems,” *IEEE J. Sel. Areas Commun.*, vol. 10, no. 8, pp. 1209–1218, Oct. 1992.
- [39] P. Larsson, “Golden angle modulation,” *IEEE Wireless Commun. Lett.*, vol. 7, no. 1, pp. 98–101, May 2017.
- [40] Q. Luo, Z. Liu, G. Chen, Y. Ma, and P. Xiao, “A novel multi-task learning empowered codebook design for downlink SCMA networks,” *IEEE Wireless Commun. Lett.*, 2022.
- [41] Y. Xin, Z. Wang, and G. B. Giannakis, “Space-time diversity systems based on linear constellation precoding,” *IEEE Trans. Wireless Commun.*, vol. 2, no. 2, pp. 294–309, Mar. 2003.
- [42] M. Chiani, D. Dardari, and M. K. Simon, “New exponential bounds and approximations for the computation of error probability in fading channels,” *IEEE Trans. Wireless Commun.*, vol. 2, no. 4, pp. 840–845, Jul. 2003.
- [43] C. Tellambura, “Evaluation of the exact union bound for trellis-coded modulations over fading channels,” *IEEE Trans. Commun.*, vol. 44, no. 12, pp. 1693–1699, Dec. 1996.
- [44] K. Zeger and A. Gersho, “Pseudo-gray coding,” *IEEE Trans. commun.*, vol. 38, no. 12, pp. 2147–2158, Dec. 1990.
- [45] Altera Innovate Asia website, Presentation, “1st 5G algorithm innovation competition-env1.0-SCMA.” [Online]. Available: <http://www.innovateasia.com/5G/en/gp2.html>.
- [46] L. Yang, Y. Liu, and Y. Siu, “Low complexity message passing algorithm for SCMA system,” *IEEE Commun. Lett.*, vol. 20, no. 12, pp. 2466–2469, Sep. 2016.
- [47] L. Deng, Z. Liu, Y. L. Guan, X. Liu, C. A. Aslam, X. Yu, and Z. Shi, “Perturbed adaptive belief propagation decoding for high-density parity-check codes,” *IEEE Trans. Commun.*, vol. 69, no. 4, pp. 2065–2079, Apr. 2021.
- [48] 3GPP TS 38.212, Rel. 15 , “5G NR, multiplexing and channel coding,” Jul. 2018. [Online]. Available: <https://www.etsi.org/deliver/etsits/138200138299/138212/15.02.0060/ts138212v150200p.pdf>